의학박사 학위논문

Cooperative role of RanBP9 and P73 in mitochondria-mediated apoptosis

미토콘드리아 매개에 의한 세포자멸사에서 RanBP9 과 P73의 협력적 역할

2014년 08월

서울대학교 대학원

의과학과 의과학전공

LIU TIAN

미토콘드리아 매개에 의한 세포자멸사에서 RanBP9 과 P73의 협력적 역할

지도교수

묵인희

이 논문을 의학박사 학위논문으로 제출함

2014년 04월

서울대학교 대학원

의과학과 의과학전공

리우티안

리우티안의 의학박사 학위논문을 인준함

2014년 06월

위 원 장 김상정 (인)

부위원장 묵인희 (인)

위 원 권용태 (인)

위 원 김만호 (인)

위 원 최철용 (인)

Cooperative role of RanBP9 and P73 in mitochondria-mediated apoptosis

by

LIU TIAN

A thesis submitted to the Department of Biomedical Scien ce in partial fulfillment of the requirements for the Degree of Doctor of Philosophy in Biomedical Science at Seoul National University College of Medicine

June, 2014

Approved by Thesis Committee:

Professor Sang Jeong Kim Chairman

Professor Inhee Mook-Jung Vice chairman

Professor Yong Tae Kwon

Professor Manho Kim

Professor Cheol Yong Choi

Abstract

Cooperative role of RanBP9 and P73 in mitochondria-mediated apoptosis

LIU TIAN

Department of Biomedical Science

The Graduate School

Seoul National University

Multiple lines of evidence indicate that the accumulation of Amyloid β (Aβ), a peptide derived from the proteolytic processing of the amyloid precursor protein (APP), plays an essential role in Alzheimer's disease (AD) pathogenesis. It has been recently demonstrated that the scaffolding protein RanBP9 robustly increases Aβ generation by promoting BACE1 cleavage of APP. In addition, RanBP9 levels are markedly increased in brains of AD patients. A recent report showed that RanBP9 potentiates DNA damage-induced apoptosis, and knockdown of RanBP9 decreases Bax protein levels. However, little is known regarding the role of RanBP9

is promoting apoptosis. In this study, overexpression of RanBP9 increases mitochondrial reactive oxygen species (ROS) and a fall in mitochondrial membrane potential (MMP). Even under conditions in which cell death could not be detected upon serum withdrawal, RanBP9 promoted cell death as measured by Annexin V and LDH release. This event was accompanied by an increase in Bax levels at the protein but not mRNA levels as well as a reduction in the anti-apoptotic Bcl-2 protein. Immunocytochemical analysis demonstrated that RanBP9 overexpression led to the distortion of mitochondrial morphology and induced cytochrome c release. Interestingly, full length RanBP9 and especially its N60 fragment elevated in AD were localized in the biochemically separated mitochondrial fraction, suggesting a direct role of RanBP9 in the mitochondria. In addition, both RanBP9- and p73α-induced apoptosis are interfered by pan-p73 siRNA and RanBP9 siRNA, respectively. Meanwhile pan-p73 siRNA rescues RanBP9-induced imbalance of Bax and Bcl2 protein level and abnormal mitochondrial fission. In HT22 cells, RanBP9 stabilizes and interacts with p73α and increases p73 level in mitochondria. In addition, RanBP9 protein level also affects p73 protein half-life. More interestingly, there is more p73 protein level in primary hippocampal neurons from RanBP9 transgenic mice than from wild-type mice. These data suggest a pathogenic role of RanBP9 co-working with

p73 in promoting apoptosis via a mitochondrial mechanism in addition to its role in increasing Aβ generation, both of which contribute to the AD pathogenic mechanism.

* This work is published in Cell Death and Disease (2013) 4, e476; doi:10.1038/cddis.2012.203; published online 24 January 2013

……

Key words: amyloid; apoptosis; RanBP9; p73; mitochondria

Student Number: 2010-31373

Contents

List of Figures

Introduction

Alzheimer's disease (AD), a type of neurodegenerative diseases, is characterized by memory loss and other cognitive functions due to the neuronal loss caused by accumulation of amyloid beta (Aβ) and hyperphosphorylated tau in the hippocampus region (Figure 1) (1, 2). Aβ plaques are found in the Alzheimer patients brains and derived from the amyloid precursor protein (APP). APP can be cleaved into three fragments by β-secretase (BACE) and γ-secretase, in which Aβ can be produced and aggregated to form plaques (3, 4). Many studies have shown that both soluble Aβ oligomers and mature fibrils have toxicity to cells, but soluble form is more toxic (5, 6). Many findings suggest that the accumulation of Aβ is an important process in the development of AD, in which Aβ induces toxicity and leads to the neuronal loss of hippocampus (7). It has been studied well how Aβ induces cell toxicity in many pathways. It has been reported that Aβ induces neuronal apoptosis through c-Jun N-terminal kinase pathways and the induction of Fas ligand (8). Aβ also can induce neuronal death via ROS-mediated ASK1 activation (7). During the Aβ-induced process, caspases activation is also increased due to the

treatment of Aβ (9). Especially, cell death induced by amyloid plaque is a rapid process due to the oxidative stress (10). Progressive cell loss is the most common type of dementia in the AD, but cellular mechanism that regulates neuronal cell death during naturally developmental death or injury-induced cell death is still not well understood. It has been generally thought Aβ contributes to neurodegeneration through the activation of an apoptotic pathway (11-14). It has been reported that Aβ localizes to mitochondrial membrane and impairs mitochondrial functions through interacting with mitochondrial proteins, disrupting electron-transport chain and increasing mitochondrial ROS product (15-17). Tau aggregation is another major hallmark of AD. Tau is the kind of protein that can stabilize microtubules and mostly found in neurons (18). Hyperphospholorylation of tau can form tangles of paired filaments and straight filaments, and their misfolded form can aggregate in the brain and contribute to the AD (19). Researchers found that in AD tau properties are changed in several ways including its abnormal hyperphosphlorylation at many sites, loss of microtubule binding, redistribution from an axonal to a somatodendritic pattern and its aggregation (20). Regarding to the pathological conditions in AD, hyperphosphlorylation of tau protein can reduce its tubulin binging capacity resulting in microtubule disorganization, and this protein also can self-polymerize and aggregate in

the form of neurofibrillary tangles, which lead to the dysfunction of neurons resulting in neuronal loss (21).

Ran, Ras-related nuclear proteins, belongs to the superfamily of GTPases (22). All receptor-mediated transports between the nucleus and the cytoplasm are regulated by Ran. Ran small GTPases, as one of the subfamilies of GTPases, are very essential for the import of proteins into the nucleus and also for RNA export through the processes of hydrolysis of GTP and dehydrolysis of GDP (Figure 2A) (23, 24). There are also Ran binding proteins(RanBP) that cooperate with Ran together to complete the hydrolysis of GTP (Figure 2B) (25). RanBP9, is one of the RanBPs, is a small GTP binding protein belonging to RAS superfamily and plays an important role in the process of translocation of RNA and proteins through the nuclear pore complex (22). It has been shown that RanBP9 can activate Ras-Erk-SRE pathway through inducing GTP-Ras association, Erk phosphorylation and interacting with MET (26), which suggests an essential role of RanBP9 in function of migration activity. Several studies indicate that RanBP9 also contributes to the regulation of various cell signaling functions, including cell adhesion and migration, microtubule regulation, as well as the regulation of gene transcription. RanBP9 can also function on the modulation of the RNA binding properities of absence of the fragile mental retardation protein through interacting with

related proteins (27). In addition, the association between RanBP9 and CD39 suggests a potential role in regulating NTPDase catalytic activity (28). RanBP9 is also a nucleocytoplasmic mediator of cell morphology regulation through the muskelin-RanBP9 complex (29). As a scaffolding protein, the role of RanBP9 has been much studied in the neurodegeneration, especially in AD. Interestingly, RanBP9 is found to be a potent regulator in APP processing through interacting with lipoprotein receptor-related protein (LRP) and BACE1 and affecting the activity of BACE1 (30). From the same group, researchers further discovered that N-terminal fragment of RanBP9 is dramatically increased in AD brains and strongly promotes Aβ generation (31). They also found that RanBP9 and its fragment promote Aβ generation by interacting with APP/BACE1/LRP (32). Recently, it is reported that RanBP9 can simultaneous block the process of cell adhesion and promote generation via speeding up the endocytosis of APP, LRP and integrin (33). The active role of RanBP9 in neuronal survival and death has also been studied. Recent study from Molecular Cancer Research shows that RanBP9 has a novel pro-apoptotic function in DNA damage–induced apoptosis through mediating Bax and Bcl2 protein levels in mitochondria (34). From the same group, researchers also reported that RanBP9 is involved in cofilin-regulated Aβ-induced apoptosis and mitochondrial dysfunction (Figure 2C) (35), even

though the mechanism of this process is not very clear. There is another report that the stability and functions of p73 are modulated by RanBP9 through its nuclear translocation and binding with the extreme COOH-terminal region of p73α (36). However, the mechanism of RanBP9-induced apoptosis through mitochondrial pathway is still much unknown.

P73, well known as a tumor suppressor, plays an essential role in the induction of apoptosis and regulation of cell cycle. P73 has a resemblant structure with p53, but they are different because of the higher level of amino-acid sequence homology of p73 (37). Similar with p53, p73 activates the same targets including Bax and puma, but it has its specific target (38). C-abl and E2F-1 are involved in p73-induced apoptosis under the stress or DNA damage (37). P73 has its isoforms including p53-like isoforms (TAP73) and anti-p53/TAP73 isoforms (Delta TAP73), and apparently TAP73 has apoptotic activity and Delta TAP73 has anti-apoptotic activity to promote cell survival (39). The signaling pathways in p73-induced apoptosis have been well studied. TAP73 can induce ER stress due to the transactivating scotin, but this pathway is weak to induce apoptosis; Another pathway is that TAP73 can directly transactivate both Bax and puma in the nucleus, then Bax and puma induce mitochondrial pathway in a fast and efficient pattern; Third, the promoter of the death receptor CD95 can be activated by TAP73 to induce apoptosis (40).

Interestingly, nonnuclear TAP73 can induce apoptosis, in which p73 protein TAP73 and its clveavage products translocate into mitochondria and directly disrupt mitochondrial function and induce apoptosis (41, 42). Regarding to the association between p73 and RanBP9, there are several important reports. The pro-apoptotic activity of TAP73 is further promoted by RanBP9 via regulating TAP73's stability and function (43).

Apoptosis is a form of programmed cell death which has sequence of events that can eliminate cells without releasing harmful substances into around area (44, 45). Apoptosis is a normal process during the development and aging to maintain cell populations, and current studies show that cells under apoptosis will die and won't recover after the initial stages of death (46). Mitochondria, as a membrane-bound organelle, are used to supply cellular energy. The active role of mitochondria in apoptosis is well studied. Researchers started to focus on mitochondrial apoptosis after finding Bcl-2 as an apoptosis regulator was present in the mitochondrial membrane (47). After that, mitochondrial apoptosis as the best known intrinsic apoptosis pathway has been much studied (48). In this pathway, cells stress from DNA damage, loss of cell survival factors or defective cell cycle promotes the release of pro-apoptotic members, such as Bax, Bak, Noxa and Puma (34). Meanwhile, anti-apoptotic proteins like Bcl2, Bcl-xl and XIAP prevent apoptosis through inhibiting

the action of pro-apoptotic proteins (49, 50). However, when the balance of activity between pro- and anti-apoptotic members is upset, the permeability of mitochondrial membrane can be lost and mitochondrial reactive oxygen species (ROS) is induced (51, 52). Many apoptogenic proteins like cytochrome c or apoptosis inducing factors are released from mitochondria to cytosol, which can activate pro-caspases to induce apoptosis (53, 54). Impaired mitochondrial functions may precipitate or cause aging and prevalent age-associated disease including neurodegeneration (55-57). It is well known that neurodegenerative diseases including AD, Parkinson's disease, Amyotrophic lateral sclerosis and Huntington's disease are all characterized by progressive and selective neuronal loss, so mitochondrial as a key regulators of cell survival and death are likely to play an important role in these diseases (58). In AD, Aβ can induce neuronal apoptosis and increase their vulnerability by increasing oxidative stresses and reducing energy availability (59, 60).

Therefore, in this study it has been aiming to find out the mechanism that how RanBP9 promotes apoptosis via mitochondrial mechanism and what the role of RanBP9 is in Aβ–induced apoptosis in hippocampus cells. It has been hypothesized that RanBP9 may regulate neuronal apoptosis and mitochondrial dysfunction through cooperating with p73 at both post-

translational and transcriptional levels (Figure 3). This is also showing an insight into the mechanism of neurodegeneration research, especially for AD.

Materials and methods

Cell culture

Wild-type and RanBP9 transgenic mice were generated (35). Mouse hippocampal primary neurons were cultured in Neurobasal medium (Invitrogen, NY, USA) supplemented with 1X B-27 supplement (Invitrogen, NY, USA) and 1X L-Glutamine (Invitrogen, NY, USA) in a humidified atmosphere of 5% CO_2 at 37℃. Medium was replaced every 2-3 days. After two weeks' culture, cells were applied to experiments. HT22 cells, mouse hippocampal neuronal cell line, were kindly provided by Dr. David Schubert (Salk Institute). 293T cell lines were provided by Dr. Inhee Mook (Seoul National University School of Medicine, Seoul, Korea). Cells were generally cultured in Dulbecco's modified Eagle's medium (DMEM, Thermo Scientific, MA, USA) supplemented with 10% fetal bovine serum (FBS, Invitrogen, NY, USA) and 1% penicillin/streptomycin (P/S, Invitrogen, NY) in a humidified atmosphere of 5% CO_2 at 37℃.

LDH release assay

HT22 cells were cultured in DMEM medium with 1% penicillin/streptomycin and 10% FBS in the 24-well plate. After 24h incubation, transfection was performed using lipofectamine 2000 referring to the manufacture's protocol. After 48h incubation, 200ul culture medium was collected used in LDH assay. LDH level was measured with In vitro Toxicology assay kit (Sigma-Aldrich, MO, USA) by spectrophotometer following the manufacture protocol.

Transient transfection

Transient transfections of HT22 cells and 293T cells with DNA plasmid carried out using lipofectamine 2000 (Invitrogen, Carlsbad, CA, USA) and Opti-MEM I (Invitrogen). For siRNA transfections, lipofectamine RNAiMAX (Invitrogen) and Opti-MEM I were applied. 4-6h following transfections, medium was replaced with new complete medium. Generally cells were incubated 48h after plasmid transfection and 72h after siRNA transfection.

DNA constructs and siRNA

pEGFP-C2-RanBP9 was a kind gift from Dr. Hideo Nishitani (Kyushu University, Fukuoka, Japan). pcDNA-P3X-Flag-RanBP9 construct was a gift from Dr. Shim S-K (Yale University School of Medicine, New Haven,

CT, USA). pLHCX RanBP9 and RanBP9-N60 constructs have previously been described (30). pCMV-XIAP, pcDNA-myc-Bcl2 and pcDNA-myc-Bcl-xl constructs were gifts from Dr. Ryu Hoon (Boston University, Boston, USA). RanBP9 siRNA was synthesized by Samchully Pharm (Korea) with the sequence as: Sense UCUUAUCAAUACCUGCTT; Antisense GCUGGUAUUGUUGAUAAGATT. Pan-p73 siRNA was synthesized by Biobeer (Korea) and its sequence was referred in (61) with the following sequence: sense 5'-CCAUCCUGUACAACUUCAUGUG-3', antisense 5'-CAUGAAGUUGUACAGGAUGGUG-3'. pcDNA-HA-p73α and DNp73α constructs were generously provided by Dr. Nakagawara (Japan).

Chemicals and antibodies

RanBP9 monoclonal antibody was produced, which was previously described (62). Anti-Flag M2 and anti-β-actin monoclonal antibodies were obtained from Sigma (St. Louis, MO, USA).

Anti-Bax (N-20), anti-Bcl2 (N-19), anti-HA-probe (Y-11), anti-p73 (H-79) and anti-p-JNK (Thr183) antibodies were purchased from Santa Cruz (CA, USA). Rabbit anti-Cytochome c antibody was obtained from Cell Signaling (Danvers, MA, USA). Mouse anti-cytochome c antibody (Clone: 6H2.B4) was purchased from BD Pharmingen (MD, USA). Anti-Timm50

antibody was purchased from Abcam (MA, USA). Secondary antibodies including Goat Anti-Mouse IgG and Goat Anti-Rabbit IgG were purchased from Jackson ImmunoResearch (West Grove, PA, USA). SP600125 was purchased from Sigma-Aldrich (MO, USA).

Cell death assay, JC-1 staining and MitoSoxRed staining

HT22 cells were cultured in the DMEM medium with 10% FBS. After washed with cold PBS, cells were stained using Annexin-V-FITC and PI Apoptosis Detection Kit (BD Bisosciences) for 20min and apoptosis was measured by FACScan flow cytometry (Becton Dickinson, San Diego, CA, USA) according to the manufacturer's instructions.

For JC-1 staining and MitoSox Red staining, after harvesting and washing cell with PBS, cells were stained with JC-1(Invitrogen) or MitoSox (Invitrogen) Red for 15min. Cells were washed once with binding buffer and measured by flow cytometry or captured by fluorescence microscopy. Quantitations were performed by selecting the cellular region of 20-30 cells for each sample and measuring the intensity of green and red signals using Nikon NIS Elements-AR software. For Annexin V cell death assay, DIV7 neurons were treated with Aβ1-42 for 24h and stained with Annexin V-FITC followed by DAPI (BD, San Diego, CA, USA).

Immunoblotting, mitochondrial isolation and Immunoprecipitation

After cells were harvested, cells lysate lysed with lysis buffer (50mM Tris-Cl,150mM NaCl, 2mM EDTA and 1% Triton-100) was obtained and total protein concentration was quantified by a colorimetric detection assay (BCA Protein Assay, Pierce, USA). Equal amounts of protein lysates were separated by sodium dodecyl sulfate–polyacrylamide gel electrophoresis on gels, and electrotransferred to Immobilon-P membranes (Millipore Corporation, Bedford, MA, USA). Interested proteins were probed by primary antibodies. The corresponding peroxidase-labeled secondary antibody was detected using ECL western blot reagents (Millipore Corporation). For Mitochondria isolation, mitochondria were isolated by Mitochondrial Isolation Kit for Cultured Cells (Thermo Scientific, IL, USA) following manual instruction. Proteins samples from both cytosol and mitochondrial fractions were separated on 12% SDS-PAGE and western immunoblotted with appropriate primary and corresponding secondary antibodies.

For immunoprecipitation experiments, 400mg of protein lysate from HT22 cells transfected with appropriate plasmids including vector, FLAG-

RanBP9, HA-p73α and DNp73α alone or in combination were precipitated with 2mg of mouse polyclonal anti-FLAG M2 antibody. Protein A/G-Sepharose beads (American Qualex, CA, USA) were added and the immune complexes were pulled down overnight at 4℃ under rotation. Beads were washed extensively with lysis buffer to remove unbound proteins and lysed by boiling in the presence of Laemmli buffer. Immunoprecipitates were subjected to SDS-PAGE, transferred to Immobilon-P membranes (Millipore), and immunoblotted using anti-HA and anti-p73 antibodies.

Quantitative real time RT–PCR

Quantitative real-time PCR (TaqMan) was performed with ABI PRISM 7700 Sequence Detection System Instrument and software (Applied Biosystems, Foster City, CA, USA), using the manufacturer's recommended conditions. Total RNA was isolated from transiently transfected cells (Trizol reagent, Invitrogen, CA), reverse transcribed (Superscript III, Invitrogen, CA), and subjected to quantitative PCR analysis using Syber green master mix (Invitrogen, CA). The comparative threshold cycle (Ct) method was used to calculate the amplification factor, and the amount of target and endogenous reference was determined from a standard curve for each experimental sample. The primer sequence of

oligonucleotides and TaqMan probes used for the analysis of Bax is: Forward 5'-CCGGCGAATTGGAGATGAACT-3'. Reverse: 5'-CCAGCCCATGATGGTTCTGAT-3'. The primer sequence of TAp73 is: Forward 5'-GCGAGGAGTCCAACATGGAT-3' and Reverse 5'-GGCACTGCTGAGCAAATTGA-3' (63). The primer sequence of GAPDH is: Forward 5'-TGTGTCCGTCGTGCATCTGA-3' and Reverse 5'-CCTGCTTCACCACCTTCTTGA-3'. P21—forward 5'-GAACTTTGACTTCGTCACGGAGA-3' and reverse 5'-CTCCGTTTTCGGCCCTGAGA-3'. Puma—forward 5'-CTCAGCCCTCCCTGTCACCA-3' and reverse 5' -GGGGAGGAGTCCCATGAAGAGA-3'.

Immunofluorescence staining

Cells were cultured on glass cloverslips coated by 100mg/l Ploy D lysine for 2h and grown for 24h. After fixing with 4% parafarmaldeyhyde, and permeabilization with 0.2% Triton-100, cells were stained with specific primary antibodies and with fluorescence-tagged secondary antibodies. Coverslips were mounted using Gel/Mount (Biomeda, CA) and observed by fluorescence or confocal microscopy (Olympus, Tokyo, Japan). Immunofluorescence for cytochrome c in primary neurons was performed by briefly treating cells with 0.01% saponin (5min on ice, which generates

holes in the plasma membrane without permeabilization, leading to the release of cytosolic content). This was followed by fixation and normal immunostaining procedures.

Annexin V and DAPI staining for fluorescence microscope

Cells were cultured on glass cloverslips coated by 100mg/l Ploy D lysine for 2h. Cells were washed by PBS once and by Annexin V binding buffer once. Then Annexin V and DAPI diluted in Annexin V binding buffer in the ratio of 1:10 and 1:1000 were directly applied to stain cells for 10 min in cell culture incubator. After washed the cells with Annexin binding buffer and added extra 1ml of this buffer, fluorescence microscopy was used to capture cells.

Results

Excessive RanBP9 induces mitochondrial membrane permeability and increases cell toxicity in HT22 cells

In the previous study, it has been reported that the overexpression of RanBP9 has effect on cell viability and increases caspases activation, and cell death is also observed due to its ectopic expression in Hellas cells (34). It was supposed that RanBP9 could also affect cell viability and induce cell apoptosis in HT22 cells. To determine RanBP9 may induce cell toxicity, Lctate Dehydrogenase (LDH) release assay was performed to measure the cytotoxicity. Figure 4A shows that both in the medium with 10% serum and 2% serum, there was more released LDH in RanBP9 transfected cells than in only vector-transfected cells. Under the condition of 2% serum, there was marked increase of LDH release in RanBP9-transfected cells than in vector-transfected cells. To determine whether RanBP9 could induce cell apoptosis in HT22 cells, Annexin V and Propidium iodide (PI) were applied to stain apoptotic cells and this staining was quantified by flow cytometry. Compared with vector transfection, the proportion of pro-apoptotic cells (low right) had a

significant increase from 21.8% in only vector-transfected cells to 45.1% in RanBP9-transfected cells (Figure 4B). Thus, the results suggest that in HT22 cells ectopic expression of RanBP9 induces cell apoptosis under stressed conditions but there is less significant cell apoptosis under normal culture conditions.

As mitochondrial oxidative stress and mitochondrial membrane potential (MMP) are the general indicators of mitochondrial health, whether ectopic RanBP9 could impact on mitochondrial MMP and ROS levels was supposed. To investigate the role of RanBP9 in mitochondrial membrane potential, JC-1, an indicator of MMP, was applied to stain cells after transfecting RanBP9 and vector. Figure 4C (upper panels) shows after transfecting RanBP9 there was a significant accumulation of monomeric JC-1 with green fluorescence. As the JC-1 dye indicates potential-dependent accumulation in mitochondria and fluorescence shift from green (529 nm) to red (590 nm), mitochondrial depolarization is indicated by a decrease in red/green fluorescence intensity ratio. Therefore, this result represented the decrease of mitochondrial membrane potential. But in only vector-transfected cells, there were only dye aggregates with red fluorescence. Flow cytometry was used to further test it. In R2 area, compared to control JC-1 monomer, there was a significant increase in RanBP9-transfected cells (Figure 4C, lower panels). To measure reactive

oxygen species (ROS) in mitochondrial, MitoSoxRed was used to stain cells after transfection. In RanBP9-transfected cells significant red fluorescence was observed, but in vector-transfected cells red fluorescence was significantly weaker (Figure 4D, upper panels). Then quantification with flow cytometry indicates that RanBP9-transfected cells show higher median fluorescence intensity value with 111 than vector-transfected cells with the intensity value of 91 (Figure 4D, lower panels). These results taken together indicate that RanBP9 increases the vulnerability of cells to undergo apoptosis and mitochondrial dysfunction even under conditions where overt cell death is not readily detectable.

Overexpression of RanBP9 affects Bax and Bcl2 protein expression levels, promotes Bax oligomerization and induces cytochrome c release

It has been shown that in Hella cells knockdown of RanBP9 by siRNA decreases mitochondrial Bax protein level and increases total Bcl2 protein level (34). To determine whether the same corresponding changes are also observed after RanBP9 overexpression in brain-derived cells, Bax and Bcl2 protein levels were analyzed after transfecting RanBP9 or control vector in HT22 cells. Compared with the control, overexpression of RanBP9 dramatically reduced Bcl2 protein level but significantly

increased Bax protein level; Compared to the condition in the medium with 10% serum, with that of serum withdrawal by 2% there was more decrease of Bcl2 but more increase of Bax protein level (Figure 5A). Bax protein level was further analyzed by immumocytochemistry after transfecting RanBP9. Figure 5B shows both in the medium with 10% serum and 2% serum, EGFP-RanBP9-transfected cells shows significantly higher Bax protein level (red) than only vector-transfected cells. After quantification, compared to vector-transfected cells, RanBP9-transfected cells show more than one-fold increase of Bax protein level in the medium with 10% serum and almost 2.5-fold increase of Bax protein level in the medium with 2% serum (Figure 5C). To determine whether overexpression of RanBP9 affected Bax in transcription dependent way, Bax mRNA level was determined after transfection of control vector and RanBP9. Figure 5D indicates that overexpression of RanBP9 did not significantly alter Bax mRNA level, indicating that the increase in Bax protein is not due to the transcriptional mechanism. To determine whether overexpression of RanBP9 induces Bax oligomerization, the monomer, dimer, and tetramer of the Bax protein were detected using anti-Bax antibody. Result shows that compared with vector-transfected cells RanBP9 transfection not only significantly increased the 23-kD monomer but also significantly increased SDS-resistant 46-kD dimer (Figure 5E),

indicating that RanBP9 promotes Bax oligomerization leading to increased mitochondrial membrane permeability.

As well known that higher Bax/Bcl2 ratio can increase Bax oligomerication, and decreased MMP leads to the release of cytochrome c which is a proapoptotic protein that promotes caspase activation and initiation of mitochondria-mediated apoptosis. To determine if overexpression of RanBP9 could induce release of cytochrome c, anti-cytochrome c (6H2.B4) antibody was used to stain cells after transfection of RanBP9 and vector. Figure 3E indicates in comparison with vector-transfected cells much more cytochrome c was observed in cytosol in EGFP-RanBP9-transfected cells (Figure 5F). It was further confirmed by detecting this protein from biochemical isolation of mitochondria and cytosolic fractions. As expected more cytochrome c protein was detected by anti-cytochrome c from cytosolic fraction with RanBP9 transfection compared with only vector-transfected cells, and there was decrease of cytochrome c in mitochondrial fraction compared to control (Figure 5G). Cytosolic cytochrome c in control vector-transfected cells was not detectable (Figure 5G). Therefore, these results suggested that overexpression of RanBP9 alters Bax/Bcl2 protein ratio, promotes Bax oligomerization, leads to the reduction of mitochondrial membrane potential, increase of mitochondrial ROS and releasing of cytochrome c

from mitochondria, all of which render cells more vulnerable to apoptosis.

RanBP9-induced fragmentation of mitochondria and apoptosis is partially prevented by inhibition of mitochondrial fission

Since it has been shown excessive RanBP9 induced mitochondrial dysfunctions, it has been wondered whether mitochondrial morphology was also affected by RanBP9 under conditions of 10 and 2% FBS. RanBP9 was co-transfected with Mito-dsRed construct which is used to stain mitochondria in HT22 cells. In comparison with vector-transfected cells, mitochondria in RanBP9-transfected cells show serious mitochondrial fragmentation and fission (Figure 6A). It also shows 2% serum-withdraw led to mitochondria fragmentation both in vector-transfected cells and RanBP9-transfected cells, and more significant aggregation of mitochondria in RanBP9-transfected cells (Figure 6A). The length of mitochondria was measured and quantified. Figure 3B shows in the medium with 10% serum mitochondria length was two-fold shorter due to RanBP9 overexpression compared to vector control; in the medium with 2% serum compared to vector control it was further shortened two-fold. In addition serum withdrawal itself also led to mitochondria shortening.

The process of mitochondrial fission mediated by DRP1 not only participates in regulating mitochondrial morphology but also is important in cell apoptosis (64). It has been reported that mdivi-1 is used to inhibit DRP1 so as to inhibit mitochondrial fission and apoptosis as well (65-67). To further determine whether RanBP9 could induce mitochondria fission, mdivi-1 was applied to treat cells after transfecting RanBP9. In comparison with vector-transfected cells mitochondrial length was shortened more than 3 folds in RanBP9-transfected cells; however, it was significantly recovered by the treatment of mdivi-1 (Figure 6C). Whether mdivi-1 could prevent RanBP9-induced apoptosis was also determined. Figure 3D shows that compared with vector control RanBP9 transfection increased the both pro- and late-apoptotic proportion from 29.1% and 11.9% to 33.1% and 26.3%, respectively; but they were decreased to 29.3% and 14.7%, respectively, due to the treatment of mdivi-1, indicating that mdivi-1 significantly prevented apoptosis and mitochondria fission induced by RanBP9 (Figure 6D). Taken together, the process of mitochondrial fission is an integral component of RanBP9-induced cell death.

Anti-apoptotic proteins XIAP, Bcl2 and Bcl-xl, suppress RanBP9-induced toxicity

X-linked inhibitor of apoptosis protein (XIAP) stops apoptotic cell death by binding and inhibiting caspases 3, 7 and 9, and by mediating translocation of Ba/x to mitochondria (68-70). Both Bcl2 and Bcl-xl are mitochondrial proteins that can inhibit apoptosis (71, 72). We have shown that RanBP9 promoted cytochrome c release and induced mitochondrial dysfunction. To further demonstrate RanBP9 induced cell apoptosis through mitochondrial pathway, XIAP, Bcl2 and Bcl-xl constructs were applied to determine whether they could inhibit RanBP9-induced apoptosis. Annexin V and PI staining was used to test cell apoptosis after co-transfecting XIAP, Bcl2 and Bcl-xl with RanBP9. Figure 7A shows that in comparison with only vector-transfection co-transfection of RanBP9 and vector increased the pro-apoptotic proportion from 22.0% to 37.2%, and increased late-apoptotic proportion (upper right) from 13.2% to 22.8%, but they were decreased to 28.1% and 10.7%, respectively, due to co-transfection of RanBP9 and XIAP. Figure 7B shows that in comparison with only vector-transfection co-transfection of RanBP9 with vector increased the pro-apoptotic proportion from 20.8% to 30.9%, and increased the late-apoptotic proportion from 12.2% to 30.2%, but the pro-apoptotic proportion was decreased to 25.4% and 20.1%, and the late-apoptotic proportion was also decreased to 19.7% and 18.5% due to co-transfection of RanBP9 and Bcl2, and co-transfection of RanBP9 and Bcl-

xl, respectively; meanwhile, late-apoptotic proportion was increased from 12.2% to 30.2%, but it was decreased again to 19.7% and 18.5% by Bcl2 and Bcl-xl, respectively. All of these results indicate that XIAP, Bcl2 and Bcl-xl prevented RanBP9-induced apoptosis. It further demonstrated that RanBP9 induces cell death via mitochondria-dependent apoptotic pathway.

RanBP9 enhances transcriptionally active p73 levels by both post-translational and transcriptional mechanisms

It has been reported that RanBP9 had ability to bound to p73 and stabilize its function in mammalian cells (36). The p73 protein and its cleaved fragments were present in/on mitochondria during apoptosis induced by tumor necrosis factor-related apoptosis-inducing ligand (TRAIL) (73). In addition, it is reported that p73 induced GRAMD4 and apoptosis via its translocation from nucleus to mitochondria (41). Since it has been shown that RanBP9 promoted cell apoptosis, the question of what the mechanism of the process was asked. Thus, determining whether RanBP9 induced apoptosis through co-working with p73 in cytosol or in mitochondria was proposed. To see if RanBP9 interacted with p73α in HT22 cells, co-immunoprecipitation experiments with anti-M2 Flag antibody after co-transfecting RanBP9 with HA-p73α were performed. Cell lysates

prepared from HT22 cells co-transfected with HA-tagged p73α and FLAG-tagged RanBP9 were immunoprecipitated by anti-M2 Flag antibody, followed by immunoblotting with anti-M2 Flag, anti-HA, anti-p73 antibodies, respectively. Figure 8A shows that Flag-RanBP9 co-immunoprecipitated with both HA-p73 and anti-p73α, suggesting the interaction between RanBP9 and p73. To determine if RanBP9 affected the total amount of endogenous p73 level, p73 from the whole lysate were detected after the transfection of RanBP9. Indeed, RanBP9 overexpression increased overall endogenous p73 protein (Figure 8B). Mitochondrial p73 after co-tranfected RanBP9 and HA-p73α were also measured. As shown in Figure 8C, co-transfection with RanBP9 and p73α significantly increased p73 protein level in mitochondria than only transfection with p73α. Since it has been demonstrated that RanBP9 induced apoptosis through mitochondrial pathway, it was still supposed that whether RanBP9 is physically present in/on mitochondria. After transfecting full length of Flag-RanBP9 and its N60 in 293T cells and HT22 cells, and isolating mitochondria, full length of RanBP9 and N60 fragment were detected by anti-M2 Flag antibody from mitochondrial fraction; it also shows that in the mitochondria, much more N60 fragment was detected more than full length RanBP9 (Figure 8H and I). Whereas the p73 protein level was affected by RanBP9 overexpression, we also supposed RanBP9

may stabilize endogenous p73, so after overexpressed and knocked down the RanBP9, HT22 cells were treated with cycloheximide (CHX) in a time-dependent manner and p73 protein levels were detected by anti-p73, indicating the increase of the half-life of p73 by RanBP9 (Figure 8D). It also indicates the stabilization of p73 by RanBP9 at the post-translational level. Previous studies have shown that RanBP9 can also act in the nucleus as a transcriptional co-regulator (74-76). It is wondered whether RanBP9 altered the level of endogenous p73 mRNA. To demonstrate this point, quantitative real-time reverse transcription (RT) PCR analysis was performed. Result shows that RanBP9 increased the level of p73 mRNA level by ~1.7-fold in HT22 cells (Figure 8E), which indicates that RanBP9 controls p73 levels and its mitochondrial content, both transcriptionally and post-translationally. To determine whether RanBP9 increases transcriptionally active p73, the levels of p21 activated by p53and puma mRNAs activated by both p53 and p73 were also assessed. Quantitative real-time RT-PCR analysis demonstrated that RanBP9 overexpression significantly increased puma but not p21 mRNA levels, consistent with a specific increase in transcriptionally active p73 but not p53 (Figures 8F and G). Taken together, RanBP9 interacted with p73α and enhances p73 activity both by post-translational and transcriptional mechanisms.

Endogenous RanBP9 and p73 cooperate to during mitochondrial dysfunction and apoptosis

So far, according to all the obtained results in this study, it has been supposed that RanBP9 may co-work with p73α to induce apoptosis. It well known that induction of p73 induces mitochondrial dysfunction and apoptosis. To determine whether p73 is essential for RanBP9-induced toxicity, first of all RanBP9 and p73 siRNA (pan-si p73) were co-transfected to see whether knockdown of p73 protein level could rescue RanBP9-induced changes of mitochondrial proteins. As shown in Figure 9A, overexpression of RanBP9 increased both p73 and Bax proteins levels and decreased Bcl2 protein level, but both of these two proteins levels were recovered after knockdown the p73 protein level using p73 siRNA. Next p73 siRNA were applied to determine whether it could also decrease RanBP9-induced apoptosis. Similarly, after co-transfection of RanBP9 and pan-p73 siRNA, cell apoptosis was performed using flow cytometry. Figure 6B shows RanBP9 increased pro-apoptotic proportion from 34.4% in only vector-transfected cells to 52.5% in RanBP9-transfected cells. Again, it was decreased to 35.5% due to co-transfection of RanBP9 and pan-p73 siRNA (Figure 9B, upper panels). To investigate if pan-p73 siRNA also rescues RanBP9-induced decrease of mitochondrial membrane potential, JC-1 were applied to stain cells after co-transfecting

RanBP9 with pan-p73 siRNA and this was quantified using flow cytometry. Result shows that after transfecting RanBP9 there was 44.4% accumulation of monomeric JC-1 compared with 27.9% accumulation of monomeric JC-1 in only vector-transfected cells. But it was decreased to 28.3% due to the co-transfection of RanBP9 and pan-p73 siRNA (Figure 9B, lower panels). Then, the question about whether abnormal cell morphology and mitochondrial fission induced by RanBP9 overexpression could also be rescued by pan-p73 siRNA was proposed. Thus, RanBP9 and mito-dsRed with pan-p73 siRNA were co-transfected and stained cells with anti-M2 Flag antibody to detect RanBP9. As shown in Figures 9C, there was significant aggregation of mitochondria in RanBP9-transfected cells, but it was much recovered due to the co-transfection with pan-P73 siRNA. The length of mitochondria were further measured and quantified. Figure 9D shows that mitochondria length was shortened two folds due to RanBP9 overexpression compared to vector control, but it was almost rescued by co-transfecting with pan-p73 siRNA. In addition, RanBP9 and DNp73α were co-transfected to determine whether it could rescue RanBP9-induced imbalance of Bax and Bcl2 protein ratio. As shown in Figure 9G, overexpression of RanBP9 increased Bax protein level but decreased Bcl2 protein level, but both of these two proteins levels were recovered after co-transfected RanBP9 and

DNp73α. Meanwhile, DNp73α were also applied to test whether DNp73α could decrease RanBP9-induced apoptosis measured by flow cytometry. Overexpression RanBP9 increased pro-apoptotic proportion from 35.4% in only vector-transfected cells to 51.1% in RanBP9-transfected cells; however, it was decreased to 42.5% again due to co-transfection of RanBP9 and DNp73α (Figure 9H).

Since it's already known RanBP9 can stabilize and interact with p73, whether RanBP9 was also required for p73-induced changed of mitochondrial proteins and apoptosis were supposed. Regarding to this point, RanBP9 siRNA and p73α were co-transfected to see whether knockdown of RanBP9 protein level could rescue p73α-induced imbalance of Bax and Bcl2 protein levels. As shown in Figure 9E, overexpression of p73α increased Bax protein level but decreased Bcl2 protein level, but both of these two proteins levels were restored by RanBP9 siRNA. Meanwhile, co-transfection of p73α and RanBP9 siRNA was performed to measure the apoptosis analyzed by flow cytometry. Figure 9F shows that p73α increased pro-apoptotic and late proportion from 26.8% and 16.1% in only vector-transfected cells to 36.7% and 28.8% in RanBP9-transfected cells, but they were decreased again to 27.3% and 20.1%, respectively, due to co-transfection of RanBP9 siRNA and p73α. This suggests that RanBP9 and p73α function cooperatively to

induce mitochondrial dysfunction and cell death. Taken together, knockdown of p73 can rescue RanBP9-induced cell apoptosis, mitochondrial dysfunctions and abnormality of mitochondrial morphology, and RanBP9 is also required in p73-induced apoptosis and imbalance of Bax and Bcl2 protein levels.

Endogenous p73 is essential for Aβ- and RanBP9-induced apoptosis and mitochondrial dysfunction in primary hippocampal neurons

Since we know there was more p73 protein level in RanBP9-transfected cells, it has been supposed that there might be the similarity in primary cell. To determine whether RanBP9 functions in a similar p73-dependent manner in inducing cell death in neurons, primary hippocampal neurons isolated from P0 pups of RanBP9 transgenic (TG) and wild-type (WT) littermates were cultured in DIV14. To this end, we did immunostaining with anti-p73 antibody in primary cells. Figure 11A shows that there was significant higher red fluorescence signal in transgenic primary cells than in wild type primary cells. After quantified the red fluorescence, compared with wild type cell there was about 2.5 folder increase of p73 protein in RanBP9 transgenic cells (Figure 11B). According to the paper previously published (35), with the treatment of Aβ, primary cells from

RanBP9 transgenic mouse showed more cell apoptosis than from wild-type mouse. It has been wondered that whether knockdown of p73 may affect Aβ-induced mitochondrial dysfunction and apoptosis in RanBP9 transgenic primary neurons. Regarding this point, applied pan-p73 siRNA was to knock down p73 and the early apoptosis was measured using Annexin V-FITC staining. Firstly we performed immunofluorescence staining for cytochrome c. RanBP9 TG neurons demonstrated significantly reduced cytochrome c fluorescence intensity which is consistent with observations in HT22 cells, (Figures 11C and D), indicative of its release from mitochondria. Moreover, RanBP9 TG neurons also showed significantly reduced red JC-1 aggregates and increased green JC-1 monomers (Figures 11E and F), indicative of reduced MMP.

And then, to test the apoptosis, DIV7 primary neurons were treated with 1 μM Aβ1-42 for 24 h with or without control siRNA (siNC) or pan-p73 siRNA (siRNAp73) transfection, and cells were then subjected to Annexin V (red) and DAPI staining (blue). Under these conditions, RanBP9 TG neurons showed significantly increased percentage of Annexin V-positive apoptotic cells compared with WT controls (Figures 11G and H). P73 siRNA significantly prevented the increase of the apoptosis induced by RanBP9 and Aβ1-42 which is consistent with observations in HT22 cells,

(Figures 11G and H). Taken together, these findings demonstrate that RanBP9 and p73α work cooperatively likely in a protein complex to mediate apoptosis in mitochondria-mediated pathway in neurons.

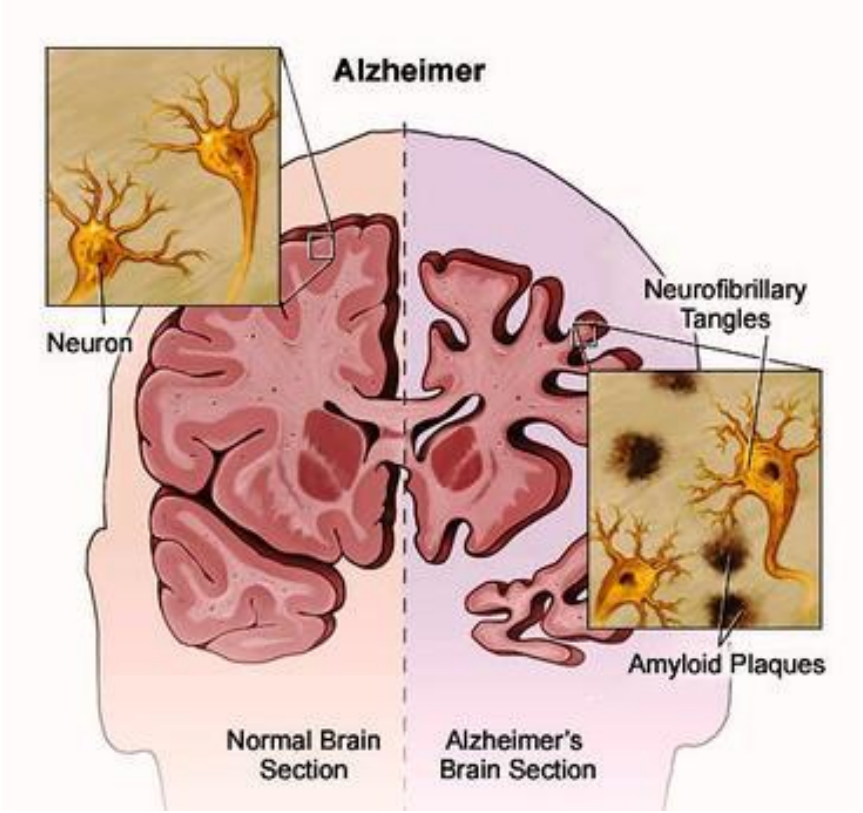

Figure 1. Schematic model of hallmark pathology of AD (Jefferson Hospital for Neuroscience). Compared to the section from the normal brain, AD brain shows the significant atrophy in the hippocampus due to the accumulation of Aβ and neurofibrillary tangles that lead to the dysfunction of neuron (2).

A

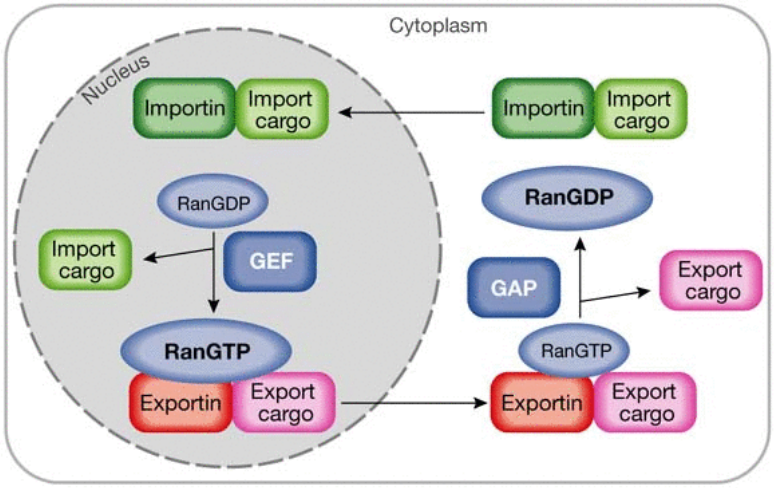
Cytoplasm
Nucleus
Importin
Import cargo
Importin
Import cargo
RanGDP
RanGDP
Import cargo
GEF
GAP
Export cargo
RanGTP
RanGTP
Exportin
Export cargo
Exportin
Export cargo

B

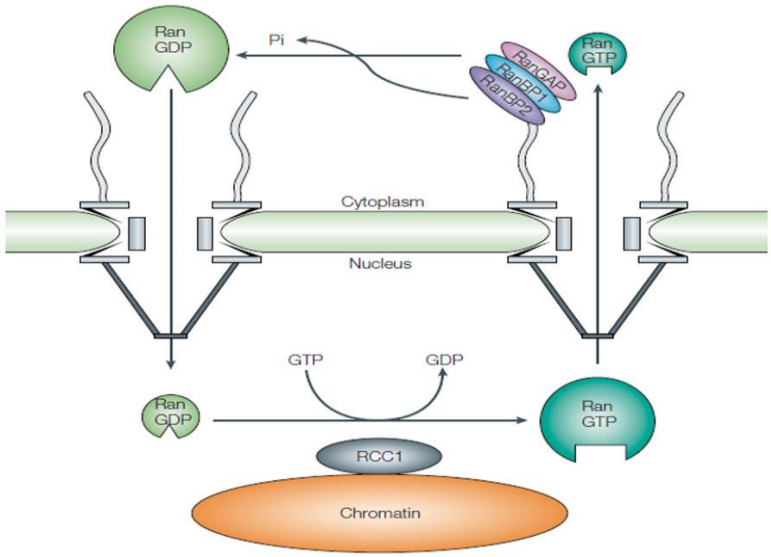
Ran GDP
Pi
RanGAP
RanBP1
RanBP2
Ran GTP
Cytoplasm
Nucleus
GTP
GDP
Ran GDP
Ran GTP
RCC1
Chromatin

C

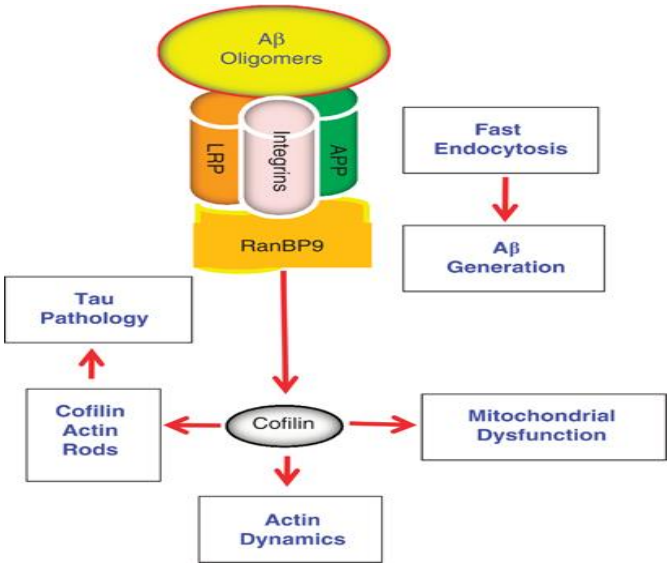

Figure 2. Ran GTPase and Ran binding proteins. (A) The role of Ran GTPases in nucleus transport. Cargos are transported through binding with Ran GTPases or GDPases; During these processes, RanGTP (RanGDP) is hydrolysed (dehydrolysed) to RanGDP (RanGTP) (24). (B) Ran binding proteins in the process of nucleocytoplasmic transport. Ran binding proteins (RanBP1 and RanBP2) cooperate with Ran to complete GTP hydrolysis in the cytoplasm (25). (C) The role of RanBP9 in AD. RanBP9 interacts with APP/LRP/Integrins complex and promotes Aβ generation via regulating the endocytosis of the complex. RanBP9 also cooperates with cofilin to regulate tau pathology, actin dynamics and mitochondrial function (35).

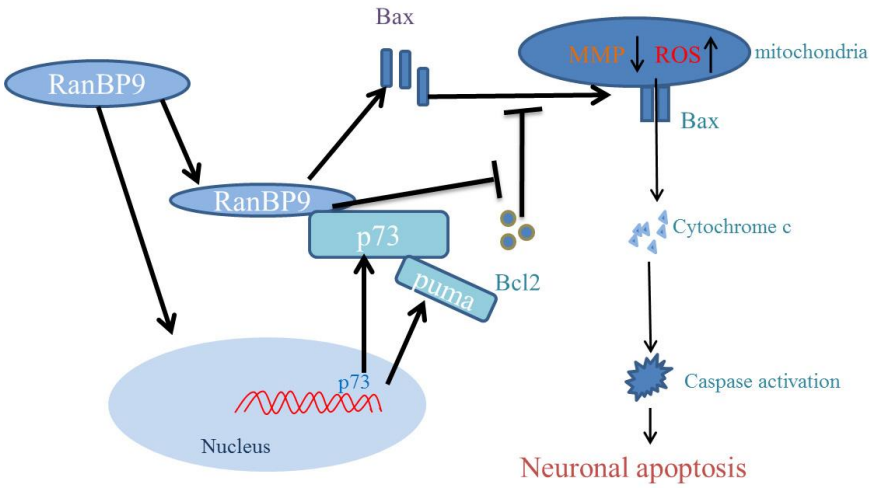

Figure 3. Hypothesis of this study. RanBP9 may cooperate with p73 to promote p73's apoptotic activity via increase p73's stability and activating transcriptionally active p73 and its target; Active p73 and its target may regulate mitochondrial apoptosis via mediating Bax and Bcl2 function, resulting in the mitochondrial dysfunction and neuronal death.

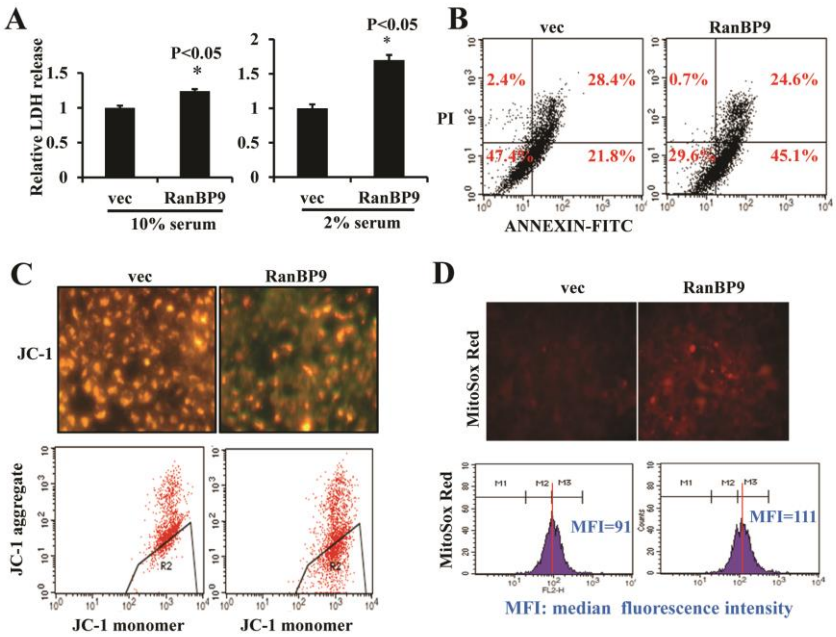

Figure 4. RanBP9 promotes cell death associated with increased mitochondrial superoxides and loss of MMP. (A) Graph illustrates a representative LDH release assay for measurement of cytotoxicity in medium collected from vector or RanBP9 transfected cells cultured with 10% and 2% serum, respectively. (n=3, each). Error bars represent S.E.M. (B) Control vector and RanBP9 were transfected in HT22 cells cultured in the medium with 2% serum. After 48h, cells were subjected in Annexin V and PI staining by flow cytometry. A representative experiment from at least three independent experiments is shown. (C) HT22 cells were transfected with vector or RanBP9. After 36 h, JC-1 staining was

performed and captured by fluorescence microscopy. Red and green fluorescence represent aggregated and monomeric JC-1. JC-1 staining was also observed by flow cytometry. Note that the R2 area represents the accumulation of monomeric JC-1 in RanBP9-transfected cells. (D) MitoSOX Red staining was performed and captured by fluorescence microscopy (upper) and flow cytometry (lower). Note the increase in the MitoSOX red signal in RanBP9 transfected cells. Representative experiments from at least three independent experiments are shown. LDH: Lactate dehydrogenase. vec: pcDNA-P3X vector control. RanBP9: pcDNA-P3X-Flag-RanBP9. N60: PLH-CX-Flag-RanBP9 N-terminal fragment. PI: Propidium iodide

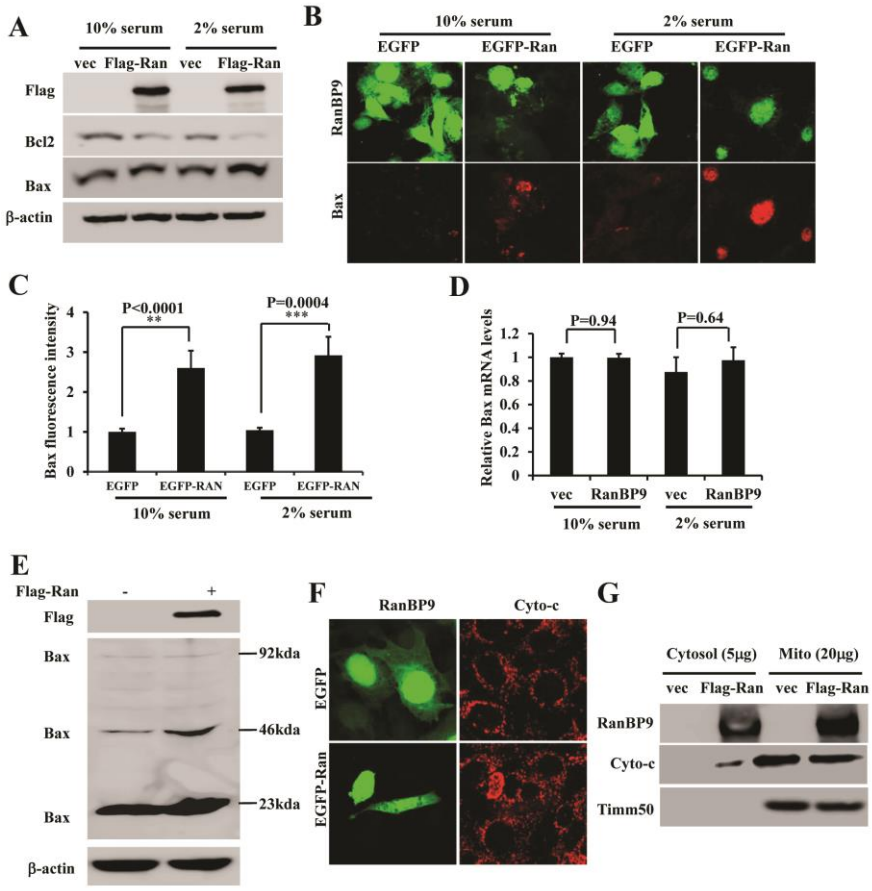

Figure 5. Increased Bax/Bcl-2 ratio and cytochrome c release in RanBP9-transfected cells. HT22 cells were transfected with vector or RanBP9 for 24 h, and cells were incubated in the medium containing 10 or 2% FBS for another 24 h. (A) Equal protein amounts of cell lysates were subjected to immunoblotting for Flag, Bax, Bcl-2 using related specific antibodies.. Note the relative decrease in Bcl-2 and increase in Bax levels in RanBP9-transfected cells. (B) HT22 cells were transfected with EGFP vector and

EGFP-RanBP9 for 24h. Cells were incubated in the medium with 10% and 2% serum for another 24h. After fixation with 4% PFA, immunflurorescence staining was subjected for Bax which was visualized by primary anti-Bax and secondary Texas Red antibodies. Images were captured by confocal microscopy. Representative images are shown. (C) Graph was made to show the quantitation of Bax immunofluorescence intensity from EGFP or EGFP-RanBP9-transfected cells (n=4 each). Error bars represent S.E.M. (D) mRNA was isolated and applied to quantitative RT-PCR by specific primer. Quantitative RT-PCR analysis of Bax mRNA levels normalized to GAPDH (n=4 each). Error bars represent S.E.M. (E) HT22 cells were transfected with vector or RanBP9 for 48 h, and equal protein amounts of cell lysates were subjected to immunoblotting for Bax. Note the increase in SDS-resistant 46-kD dimeric bax induced by RanBP9 transfection. (F) Thirty-six hours after transfection of EGFP or EGFP-RanBP9, HT22 cells cultured in 10% FBS were subjected to immunofluorescence for cytochrome c. A representative image shows widespread diffuse cytochrome c staining in EGFP-RanBP9-transfected cells, suggestive of release to cytosol. (G) Thirty-six hours after transfection of EGFP or EGFP-RanBP9, HT22 cells cultured in 10% FBS were subjected to biochemical isolation of mitochondria and cytosol. Representative experiment shows the localization of RanBP9 in both

cytosol and mitochondria as well as release of cytochrome c from mitochondria to cytosol in RanBP9-transfected cells. Timm50 was used as a marker of mitochondria.

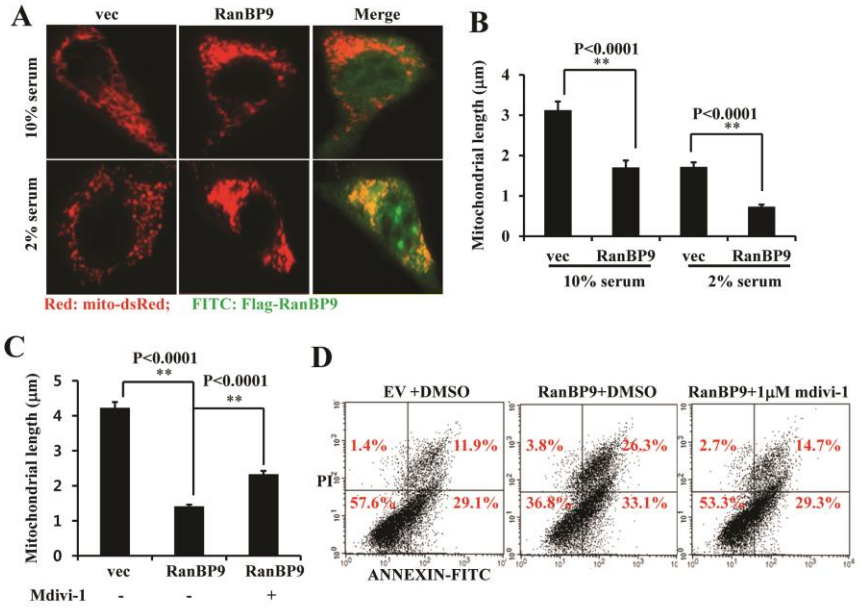

Figure 6. Inhibition of RanBP9-induced mitochondrial fission reduces cell death. (A) Flag-RanBP9 and control vector were co-transfected with Mito-dsRed in HT22 cells for 24h. Culture medium was replaced by new medium with 10% and 2% FBS, respectively. After cells were incubated for another 24h, cells were fixed with 4% PFA and immunofluorescence staining was performed for RanBP9 which was visualized by primary anti-M2 Flag and secondary Alexa 488 antibodies. Cells were captured by fluorescence microscope. Representative images show increased fragment of mitochondria (mito-dsRed) in RanBP9-transfected cells, which is further fragmented in 2% FBS. (B) Mitochondrial length was measured and quantified using NIS-Elements AR 3.2 software for (A). (n=4, each).

Error bars represent S.E.M. At least 10 cells were selected in each sample and about 50 mitochondria were measured from each selected cell. (C, D) Cells were treated with mdivi-1 with the final concentration of 5uM, and DMSO was used as negative control. After 24h cells were fixed and visualized by primary anti-M2 Flag and secondary Alexa 488 antibodies. Cells were captured by fluorescence microscope. Mitochondrial length was measured and quantified using NIS-Elements AR 3.2 software. (n=3, each). Error bars represent S.E.M. Experiments were reproduced from three independent experiments. In each experiment, 10 cells were selected in each sample and about 50 mitochondria were measured from each selected cell. Alternatively, after 24h transfection of RanBP9 and vector in HT22 cells, cells were treated with DMSO, 5μM mdivi-1 for 12h. Cells were stained by Annexin V and PI, and apoptosis was measured using flow cytometry. A representative cell death experiment is shown from at least three independent experiments.

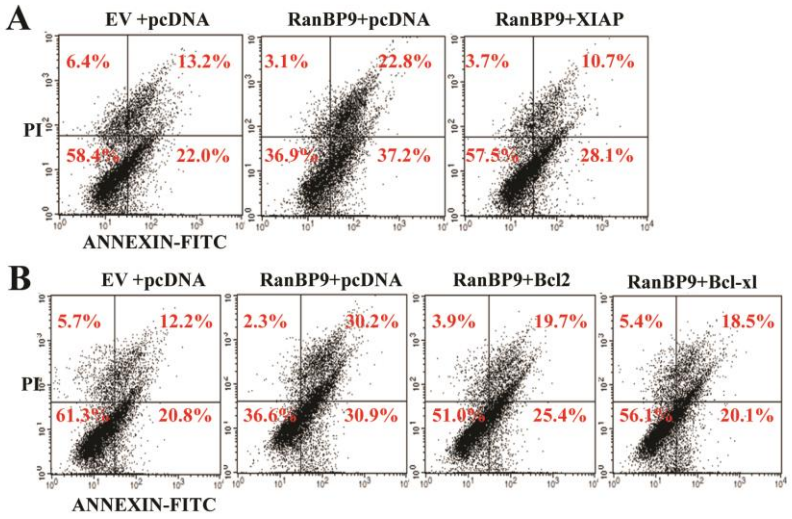

Figure 7. XIAP, Bcl-2 and Bcl-xl antagonize RanBP9-induced cell death. RanBP9 were co-transfected with vector, XIAP (A), Bcl2 and Bcl-xl (B), respectively. After 24h, medium was replaced with new medium with 2% serum. After 24h, cells were stained by Annexin V and PI, and apoptosis was measured using flow cytometry. Each independent experiment was reproduced at least three times. Representative experiments are shown.

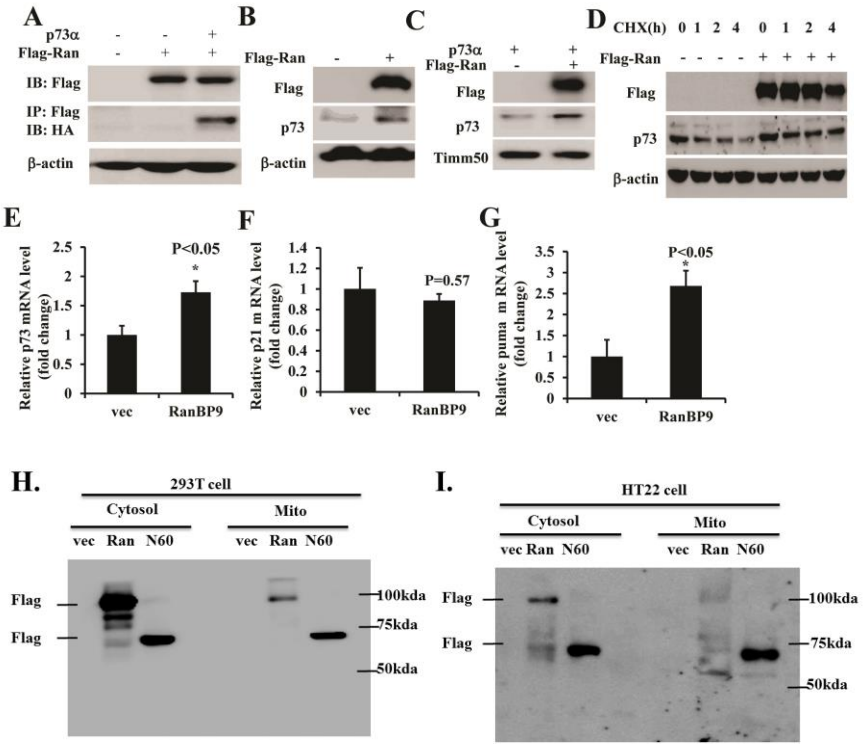

Figure 8. RanBP9 physically interacts with p73 and increases p73 levels by both protein stabilization and increased transcription. (A) FLAG-RanBP9 was co-transfected with vector and HA-p73α, respectively. Cell lysate was immunoprecipitated by anti-M2 Flag antibody and immunoblotted with anti-HA and anti-p73 antibodies. Cells lysate without immunoprecipitation was directly immunoblotted using anti-M2 Flag and anti-β-actin antibodies. (B) Vector and RanBP9 were transfected in HT22 cells. After 48h, the same amount of cell lysate was subjected in immunoblotting using anti-M2 Flag, anti-p73 and anti-β-actin antibodies.

(C) P73α was co-transfected with vector and RanBP9, respectively. After 48h, mitochondria were isolated. Mitochondrial lysate was immunoblotted using anti-M2 Flag, anti-p73 and anti-timm50 antibodies. (D) RanBP9 and vector were transfected in HT22 cells, respectively. After 48h, cells were treated with cycloheximide (CHX) with the final concentration of 2μg/ml for 0h, 1h, 2h and 4h, respectively. The same amounts of cell lysate were subjected in immunoblotting using anti-M2 Flag, anti-p73 and anti-β-actin antibodies. (E, F, G) Vector and RanBP9 were transfected in HT22 cells. After 48h, mRNA was isolated and applied to quantitative RT-PCR by specific TAp73, p21, and puma primers, and normalized to GAPDH (n=4 each). (n=4, each). Error bars represent S.E.M. (H, I) Vector, Flag-RanBP9 and Flag-N60 were transfected in 293T cells and HT22 cells. After 48 h, mitochondria were isolated, and equal protein amounts of lysates from cytosol and mitochondria were immunoblotted using anti-M2 Flag.

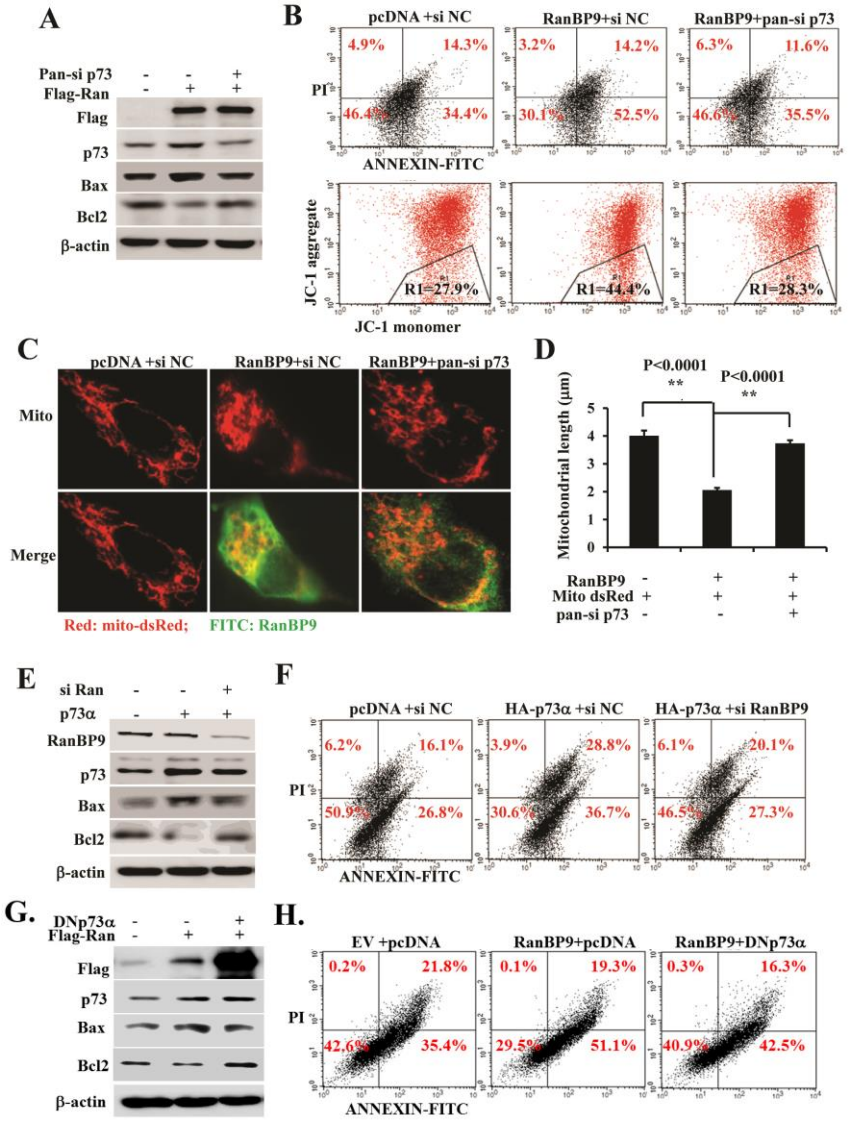

Figure 9. p73 and RanBP9 function cooperatively to induce mitochondrial dysfunction and cell death. RanBP9 was co-transfected with negative control of siRNA and pan-p73siRNA, respectively. After 48h, medium was replaced with new medium with 2% serum. (A) After

24h, the same amounts of cell lysate were subjected in immunoblotting using anti-M2 Flag, anti-p73, anti-Bax, anti-Bcl2 and anti-β-actin antibodies; (B) or after 24h, cells were stained by Annexin V and PI and apoptosis was measured using flow cytometry; or after 2h, cells were stained by JC-1, and aggregated and monomeric JC-1 were measured using flow cytometry. (C) RanBP9 and Mito-dsRed were co-transfected with negative control of siRNA and pan-p73siRNA, respectively. After 72h, cells were fixed with 4% PFA and immunoflurorescent staining was performed for RanBP9 which was visualized by primary anti-M2 Flag and secondary Alexa 488 antibodies. Cells were captured by confocal microscopy. (D) Mitochondrial length was measured using Nikon NIS Elements-AR software from at least 10 cells per sample and about 50 mitochondria per selected cell. Error bars represent S.E.M. (n=4 samples each). (E, F) HA-p73α was co-transfected with control siRNA (si NC) or RanBP9 siRNA (si RanBP9 for 72 h) in HT22 cells, and equal protein amounts of cell lysates were immunoblotted for endogenous RanBP9, p73, Bax, Bcl-2, and β-actin. Cells were also stained with Annexin V-FITC/PI and subjected to FACS analysis for cell death. A representative experiment is shown from at least three independent experiments. RanBP9 was co-transfected with vector and DNp73α. After 24h, medium was replaced with new medium with 2% serum. (G) After another 24h, the

same amounts of cell lysate were subjected in immunoblotting using anti-M2 Flag, anti-p73, anti-Bax, anti-Bcl2 and anti-β-actin antibodies; (H) Cells were also stained with Annexin V-FITC/PI and subjected to FACS analysis for cell death. A representative experiment is shown from at least three independent experiments.

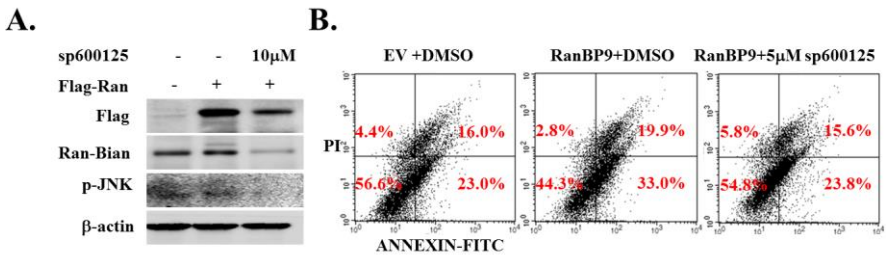

Figure 10. RanBP9 expression and RanBP9-induced apoptosis are prevented by JNK inhibitor. Vector and RanBP9 were transfected in HT22 cells, respectively. After 24h, medium was replaced with new medium with 2% serum. (A) After cells were treated by 10μM sp600125 or DMSO for another 24h, the same amounts of cell lysate were subjected in immunoblotting using anti-M2 Flag, anti-Ran-Bian (anti-RanBP9), anti-p-JNK and anti-β-actin antibodies; (B) After cells were treated by 5μM sp600125 or DMSO for another 24h, cells were stained by Annexin V and PI, and apoptosis was measured using flow cytometry. A representative experiment is shown from at least three independent experiments.

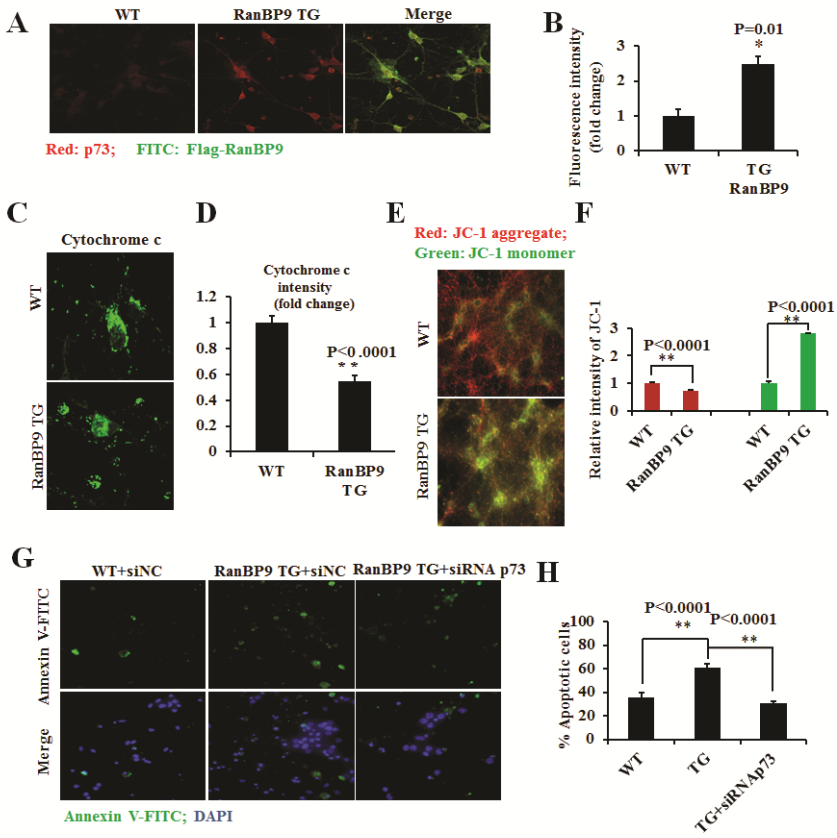

Figure 11. p73 and RanBP9 function cooperatively to induce mitochondrial dysfunction and cell death. (A) wild-type and RanBP9 transgenic littermate hippocampal primary neurons were subjected to immunostaining using anti-M2 Flag and anti-p73 antibodies. Cells were captured by confocal microscopy. (B) Red fluorescence intensity from (A) was quantified using NIS-Elements AR 3.2 software and relative quantification was shown in the graph. N=4. Error bars represent S.E.M. (C, D) RanBP9 transgenic (TG) and littermate non-transgenic (WT)

DIV14 primary hippocampal neurons were treated with 0.1% saponin (5 min on ice) to release cytosolic content prior to fixation and subjected to immunostaining using anti-cytochrome c, and images were captured by confocal microscopy. Representative images are shown. (D) Endogenous cytochrome c (FITC) intensities were quantified using Nikon NIS-Elements-AR software (n=4 each). Error bars represent S.E.M. (E, F) Wild-type and RanBP9 transgenic littermate hippocampal primary neurons were subjected to JC-1 staining prior to fixation, and JC-1 signals were captured by fluorescence microscopy. (F) Red (JC-1 aggregate) and green (JC-1 monomer) fluorescence intensities from were quantified using NIS-Elements AR 3.2 software and relative quantifications are shown in the graph (n=4 each). Error bars represent S.E.M. (G) Wild-type and RanBP9 transgenic littermate hippocampal primary neurons were transfected with p73 siNRA and negative control. After 48h, cells were treated with 1μM Aβ for 24h and were subjected to staining with Annexin V-FITC and DAPI. Cells were captured directly using fluorescence microscope. (H) Cell numbers were counted using NIS-Elements AR 3.2 software according to Annexin V-FITC positive cells and DAPI positive cells. The graph was made to show the ratio of Annexin V-FITC positive cells to DAPI-positive cells. N=3. Error bars represent S.E.M.

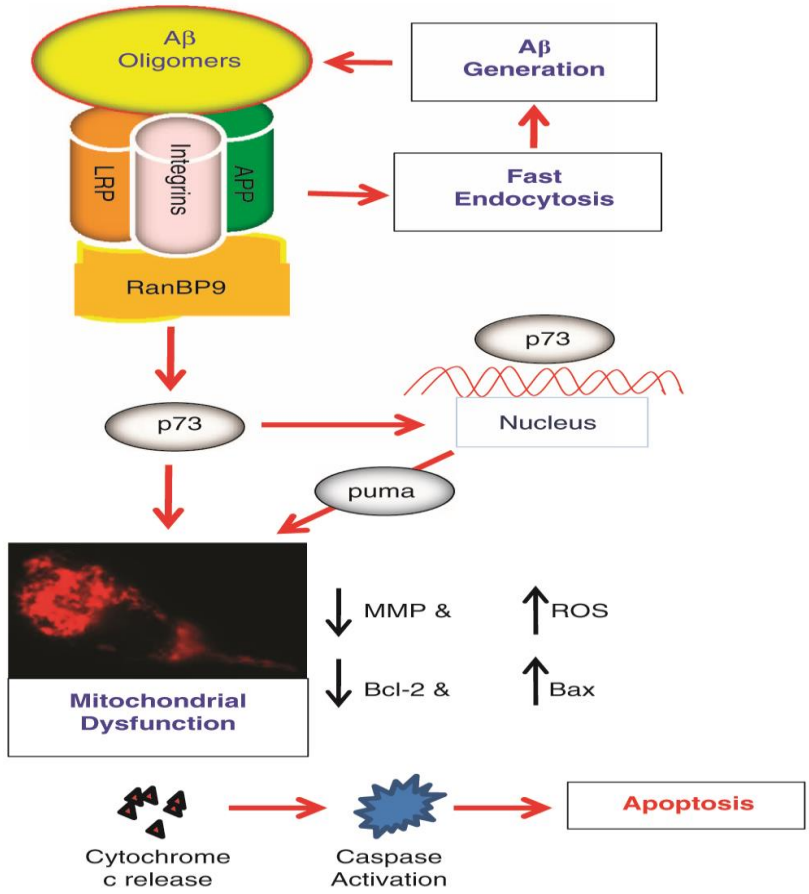

Figure 12. Schematic model of the RanBP9/p73 pathway in neurodegeneration and AD pathogenesis. As RanBP9 levels are elevated in brains of AD patients, the binding of RanBP9 to integrin/APP/LRP complexes accelerates their endocytosis, thereby simultaneously promoting Aβ generation and disrupting focal adhesions. Aβ oligomers via binding to integrin complexes further propagate their toxic signals(33,

35). Meanwhile, Aβ and RanBP9 function to stabilize p73α and/or activate its transcription. p73 translocates into the nucleus and mitochondria to induce puma, increase Bax, reduce Bcl-2, drop MMP, and enhance mitochondrial ROS, leading to increased mitochondrial permeability, release of cytochrome c, and apoptosis.

Discussion

In many neurodegenerative diseases including AD, mitochondrial dysfunction is the most common factor that leads to the neuronal loss in different region of brains. In AD, aggregations of Aβ and tau are both the most essential causal factors to induce mitochondrial dysfunction following different pathways (77). In previous studies, it has been shown that the overall levels of RanBP9 are dramatically increased in brains of AD patients and APP transgenic mice, and increased RanBP9 promotes Aβ generation both in cultured cells and in brain (Figure 12) (30, 31, 78). In current study, a series of novel findings implicate the cooperative role of the RanBP9/p73 complex in mitochondrial dysfunction and apoptosis. First, the drop of MMP and mitochondrial ROS levels were induced by RanBP9 even under conditions in which overt cell death was not readily detected. Such changes were associated with Bax protein induction and oligomerization, Bcl-2 reduction, and release of cytochrome c from mitochondria. Second, excessive RanBP9 led to the fragmentation of mitochondria and cell death, which were significantly restored by the mitochondrial fission inhibitor Mdivi-1. Third, RanBP9-induced apoptosis was efficiently blocked by classical inhibitors of mitochondrial cell death

pathway, XIAP, Bcl-2, and Bcl-xl. Fourth, RanBP9 increased endogenous p73 levels and promoted p73 localization in mitochondria by both transcriptional and post-translational mechanisms. Fifth, RanBP9 increased transcriptionally active p73 as evidenced by increased transcription of the p73 target gene, puma. Sixth, knockdown of endogenous p73 by siRNA effectively prevented RanBP9-induced changes in cell death, MMP, and mitochondrial fragmentation, indicating that p73 is an essential component of RanBP9-induced apoptosis. Seventh, RanBP9 increased p73 levels and cytochrome c release primary hippocampal neurons, and siRNA knockdown of p73 also prevented RanBP9/Aβ1-42 induced apoptosis in primary neurons. Finally, siRNA knockdown of endogenous RanBP9 was also effective in suppressing p73-induced apoptosis, suggesting cooperative roles of RanBP9 and p73 in the process of inducing cell death. Taken together, these finding implicate the RanBP9/p73 complex in mitochondrial dysfunction and apoptotic mechanisms during neurodegeneration.

One key paper has reported that RanBP9 has pro-apoptotic role in DNA damage-induced cell death pathway. However, there is still much unknown about how RanBP9 is involved in this pathway and what the association between RanBP9 and mitochondrial functions is. Previous study show RanBP9, especially its N-terminal region, dramatically

promotes A beta generation (32, 62). A very recent paper shows that RanBP9 promotes Aβ-induced neurotoxicity. It was supposed that whether it also contributes to neuron loss. In this study, overexpression of RanBP9 inHT22 cells induced toxicity. Compared with the complete medium, serum-withdrawal promoted this process. Through FACS analysis, overexpression of RanBP9, as well as its N-terminal region, significantly increased pro-apoptotic proportion. Since it has been reported that knockdown of RanBP9 reduced mitochondrial Bax protein level and increased Bcl2 protein level, both total and mitochondrial Bax and Bcl2 protein level were further determined after overexpressing RanBP9. Interestingly, both total and mitochondrial Bax protein levels were increased. In contrast, both total and mitochondrial Bcl2 protein levels were decreased. Next, to determine if Bax level was induced through transcription dependent pathway, quantitative PCR was performed to measure Bax mRNA level, but there was not significant change due to overexpression of RanBP9. Thus, it suggests that RanBP9 induced Bax level in transcription-independent pathway. It is likely that changes of Bax in total and mitochondria may affect mitochondrial function. As expected, mitochondrial membrane potential was decreased measured by JC-1, and mitochondrial ROS was significantly increased measured by mitoSoxRed staining. Cytochrome c was also released due to

overexpression of RanBP9 detected through mitochondrial isolation and immunofluorescence. To further demonstrate this hypothesis, XIAP, Bcl2 and Bcl-xl these anti-apoptotic proteins were applied. Notably, all of them can inhibit RanBP9-induced apoptosis. Meanwhile, excessive RanBP9 also changed mitochondrial morphology and induced mitochondrial fission. Then mdivi-1 which not only inhibited DRP1 protein but also inhibit apoptosis via mitochondrial pathway (66) were applied. It consists to the results that shown mdivi-1 recovered mitochondrial length and decreased RanBP9-induced apoptosis, suggesting that RanBP9 induces apoptosis via mitochondrial pathway.

In addition, it was also found that JNK inhibitor not only inhibits both extraneous and endogenous RanBP9 protein expression but also prevents RanBP9-induced apoptosis (Figure 10), indicating another pathway of RanBP9-induced apoptosis and clues for discovering the mechanism of regulation of RanBP9. JNK signaling plays an essential role in mitochondrial apoptosis, in which JNKs regulate apoptotic genes via transactivating specific transcription factors (79). So, whether JNK signaling works on regulating of the transcription of RanBP9 will be an interesting question for further exploring. Meanwhile, it also helps develop the drugs for inhibiting RanBP9 transcription, which might be a potential therapeutic strategy to treat the AD or other neurodegenerative

diseases.

Since it has been demonstrated that RanBP9 promotes apoptosis via mitochondrial pathway, it has been trying to find out the mechanism of this process in this study. It has been supposed that RanBP9, as a scaffolding protein, may interact with Bax so as to regulate its level in total or mitochondria, unfortunately, the interaction between them could not be detected using immnuoprecipitation (data not shown). However, RanBP9 and its fragment proteins in mitochondria were detected. Notably, according to immunochemistry data, RanBP9 and N60 partially localized to mitochondria. It may suggest that RanBP9 induced mitochondrial dysfunction through localizing to mitochondria. Meanwhile, p73, as a very important protein to induce apoptosis, was considered as a closed partner with RanBP9 to induce apoptosis and mitochondrial dysfunction. Recent studies show p73 is detected in mitochondria and it regulates cell death through both transcriptional and mitochondrial pathway (41, 73, 80). It is also reported that p73 physically interacts with RanBP9 and is stabilized by RanBP9, and RanBP9 promotes p73-induced apoptosis in Hela cells (36). In this study, interaction between RanBP9 was also present in HT22 cells. Notably, p73 protein level was increased both in mitochondria and in total due to overexpression of RanBP9, and RanBP9 protein level also affected p73's half-life, indicating the increase of

stability by RanBP9.

To further determine the role p73 to RanBP9-induced apoptosis, pan-p73 siRNA were applied to knock down its protein level. Interestingly, it significantly rescued RanBP9-induced apoptosis to a control level. In following study, it is also found that knockdown of p73 not only can rescue Bax and Bcl2 protein level, but also can recover mitochondrial membrane potential, mitochondrial morphology and fission induced by RanBP9 overexpression. In addition, co-transfection of RanBP9 and DNp73α also significantly decreased RanBP9-induced apoptosis. All of these suggest p73 is required for RanBP9-induced apoptosis. Since it is well known that p73α can induce apoptosis, it has been wondered whether RanBP9 is also required for p73-induced apoptosis. Thus, RanBP9 siRNA were used to co-transfect with p73α. According to the data, p73α-induced apoptosis was also reduced by RanBP9 siRNA, and both Bax and Bcl2 protein levels were also rescued. At last the p73 levels in primary cells from RanBP9 transgenic and wild-type mouse were measured and data show that there was significant increase of p73 protein in RanBP9 transgenic brain. Meanwhile, pan-p73 siRNA were also applied to knock down p73 in primary cells from wild-type and RanBP9 transgenic mouse. After the treatment with Aβ, the pan-p73 siRNA also rescued RanBP9-promoted and Aβ-induced apoptosis in primary neurons. Taken together,

RanBP9 and p73α cooperate to regulate cell apoptosis via mitochondria mechanism, but what exactly happened to them in mitochondria still need be further studied. Since RanBP9 affects Aβ generation and it is also reported p73 isoforms also play the role in neuronal development, neuronal protection and neurodegeneration (81-85), further studies on conjunctions of RanBP9 and p73 in AD and other neurodegenerative disorders in adult brain are needed and essential. Since it has been found that RanBP9 cooperates with cofilin to regulate mitochondrial dysfunction, whether cofilin might belong to the complex of RanBP9/P73 needs to be further explored. In addition, it has been previously shown that RanBP9 promotes Aβ generation in AD, but whether p73 and RanBP9 might also cooperate to promote Aβ generation remains to be determined.

RanBP9, as one of Ran binding proteins, it is likely to function on nuclear transport during the process of apoptosis. And in this study it has been discovered that p73, also well known as a nuclear transcriptional factor, is transclocated into the nucleus and induces puma transcription through cooperating with RanBP9. However, how p73 is transported into the nucleus under the condition of RanBP9 transfection is still unknown. The further actions processed in the nucleus between RanBP9 and p73 also need to be explored. On the another hand, the post-translational mechanism that p73stability is enhanced by RanBP9 via their physical

interaction association, but their interacting domains and whether the amino acids of p73 have been modified by RanBP9 or its fragments are still unknown.

References

1. Huang Y, Mucke L. Alzheimer mechanisms and therapeutic strategies. Cell. 2012;148(6):1204-22.
2. McKhann G, Drachman D, Folstein M, Katzman R, Price D, Stadlan EM. Clinical diagnosis of Alzheimer's disease: report of the NINCDS-ADRDA Work Group under the auspices of Department of Health and Human Services Task Force on Alzheimer's Disease. Neurology. 1984;34(7):939-44.
3. Li T, Huang Y, Jin S, Ye L, Rong N, Yang X, et al. Gamma-secretase modulators do not induce Abeta-rebound and accumulation of beta-C-terminal fragment. Journal of neurochemistry. 2012;121(2):277-86.
4. Sun X, Wang Y, Qing H, Christensen MA, Liu Y, Zhou W, et al. Distinct transcriptional regulation and function of the human BACE2 and BACE1 genes. Faseb J. 2005;19(7):739-49.
5. Thapa A, Woo ER, Chi EY, Sharoar MG, Jin HG, Shin SY, et al. Biflavonoids Are Superior to Monoflavonoids in Inhibiting Amyloid-beta Toxicity and Fibrillogenesis via Accumulation of Nontoxic Oligomer-like Structures. Biochemistry-Us. 2011;50(13):2445-55.
6. Lu JX, Qiang W, Yau WM, Schwieters CD, Meredith SC, Tycko R. Molecular structure of beta-amyloid fibrils in Alzheimer's disease brain tissue. Cell. 2013;154(6):1257-68.
7. Kadowaki H, Nishitoh H, Urano F, Sadamitsu C, Matsuzawa A, Takeda K, et al. Amyloid beta induces neuronal cell death through ROS-mediated ASK1 activation. Cell Death Differ. 2005;12(1):19-24.
8. Morishima Y, Gotoh Y, Zieg J, Barrett T, Takano H, Flavell R, et al. Beta-amyloid induces neuronal apoptosis via a mechanism

that involves the c-Jun N-terminal kinase pathway and the induction of Fas ligand. J Neurosci. 2001;21(19):7551-60.

9. Troy CM, Rabacchi SA, Friedman WJ, Frappier TF, Brown K, Shelanski ML. Caspase-2 mediates neuronal cell death induced by beta-amyloid. J Neurosci. 2000;20(4):1386-92.

10. Xie H, Hou S, Jiang J, Sekutowicz M, Kelly J, Bacskai BJ. Rapid cell death is preceded by amyloid plaque-mediated oxidative stress. Proc Natl Acad Sci U S A. 2013;110(19):7904-9.

11. Loo DT, Copani A, Pike CJ, Whittemore ER, Walencewicz AJ, Cotman CW. Apoptosis is induced by beta-amyloid in cultured central nervous system neurons. Proc Natl Acad Sci U S A. 1993;90(17):7951-5.

12. Kajkowski EM, Lo CF, Ning X, Walker S, Sofia HJ, Wang W, et al. beta -Amyloid peptide-induced apoptosis regulated by a novel protein containing a g protein activation module. J Biol Chem. 2001;276(22):18748-56.

13. Nelson TJ, Alkon DL. Protection against beta-amyloid-induced apoptosis by peptides interacting with beta-amyloid. J Biol Chem. 2007;282(43):31238-49.

14. Li YP, Bushnell AF, Lee CM, Perlmutter LS, Wong SK. Beta-amyloid induces apoptosis in human-derived neurotypic SH-SY5Y cells. Brain Res. 1996;738(2):196-204.

15. Reddy PH, Beal MF. Amyloid beta, mitochondrial dysfunction and synaptic damage: implications for cognitive decline in aging and Alzheimer's disease. Trends Mol Med. 2008;14(2):45-53.

16. Abramov AY, Canevari L, Duchen MR. Beta-amyloid peptides induce mitochondrial dysfunction and oxidative stress in astrocytes and death of neurons through activation of NADPH oxidase. J Neurosci. 2004;24(2):565-75.

17. Dragicevic N, Mamcarz M, Zhu Y, Buzzeo R, Tan J, Arendash

GW, et al. Mitochondrial amyloid-beta levels are associated with the extent of mitochondrial dysfunction in different brain regions and the degree of cognitive impairment in Alzheimer's transgenic mice. J Alzheimers Dis. 2010;20 Suppl 2:S535-50.

18. Avila J, Lucas JJ, Perez M, Hernandez F. Role of tau protein in both physiological and pathological conditions. Physiol Rev. 2004;84(2):361-84.

19. Alonso AD, Zaidi T, Novak M, Grundke-Iqbal I, Iqbal K. Hyperphosphorylation induces self-assembly of tau into tangles of paired helical filaments/straight filaments. Proc Natl Acad Sci U S A. 2001;98(12):6923-8.

20. Mandelkow EM, Mandelkow E. Tau in Alzheimer's disease. Trends in cell biology. 1998;8(11):425-7.

21. Kolarova M, Garcia-Sierra F, Bartos A, Ricny J, Ripova D. Structure and pathology of tau protein in Alzheimer disease. International journal of Alzheimer's disease. 2012:731526.

22. Nakamura M, Masuda H, Horii J, Kuma K, Yokoyama N, Ohba T, et al. When overexpressed, a novel centrosomal protein, RanBPM, causes ectopic microtubule nucleation similar to gamma-tubulin. The Journal of cell biology. 1998;143(4):1041-52.

23. Steggerda SM, Paschal BM. Regulation of nuclear import and export by the GTPase Ran. International review of cytology. 2002;217:41-91.

24. Corbett AH, Krebber H. Hot trends erupting in the nuclear transport field. Workshop on mechanisms of nuclear transport. EMBO reports. 2004;5(5):453-8.

25. Fahrenkrog B, Aebi U. The nuclear pore complex: nucleocytoplasmic transport and beyond. Nature reviews Molecular cell biology. 2003;4(10):757-66.

26. Wang D, Li Z, Messing EM, Wu G. Activation of Ras/Erk pathway by a novel MET-interacting protein RanBPM. J Biol Chem. 2002;277(39):36216-22.
27. Menon RP, Gibson TJ, Pastore A. The C terminus of fragile X mental retardation protein interacts with the multi-domain Ran-binding protein in the microtubule-organising centre. Journal of molecular biology. 2004;343(1):43-53.
28. Wu Y, Sun X, Kaczmarek E, Dwyer KM, Bianchi E, Usheva A, et al. RanBPM associates with CD39 and modulates ecto-nucleotidase activity. Biochem J. 2006;396(1):23-30.
29. Valiyaveettil M, Bentley AA, Gursahaney P, Hussien R, Chakravarti R, Kureishy N, et al. Novel role of the muskelin-RanBP9 complex as a nucleocytoplasmic mediator of cell morphology regulation. Journal of Cell Biology. 2008;182(4):727-39.
30. Lakshmana MK, Yoon IS, Chen E, Bianchi E, Koo EH, Kang DE. Novel Role of RanBP9 in BACE1 Processing of Amyloid Precursor Protein and Amyloid beta Peptide Generation. Journal of Biological Chemistry. 2009;284(18):11863-72.
31. Lakshmana MK, Chung JY, Wickramarachchi S, Tak E, Bianchi E, Koo EH, et al. A fragment of the scaffolding protein RanBP9 is increased in Alzheimer's disease brains and strongly potentiates amyloid-beta peptide generation. Faseb Journal. 2010;24(1):119-27.
32. Lakshmana MK, Yoon IS, Chen E, Bianchi E, Koo EH, Kang DE. Novel role of RanBP9 in BACE1 processing of amyloid precursor protein and amyloid beta peptide generation. J Biol Chem. 2009;284(18):11863-72.
33. Woo JA, Roh SE, Lakshmana MK, Kang DE. Pivotal role of RanBP9 in integrin-dependent focal adhesion signaling and assembly. Faseb Journal. 2012;26(4):1672-81.

34. Atabakhsh E, Bryce DM, Lefebvre KJ, Schild-Poulter C. RanBPM has proapoptotic activities that regulate cell death pathways in response to DNA damage. Mol Cancer Res. 2009;7(12):1962-72.
35. Woo JA, Jung AR, Lakshmana MK, Bedrossian A, Lim Y, Bu JH, et al. Pivotal role of the RanBP9-cofilin pathway in Abeta-induced apoptosis and neurodegeneration. Cell Death Differ. 2012;19:1413-23.
36. Kramer S, Ozaki T, Miyazaki K, Kato C, Hanamoto T, Nakagawara A. Protein stability and function of p73 are modulated by a physical interaction with RanBPM in mammalian cultured cells. Oncogene. 2005;24(5):938-44.
37. Huqun, Endo Y, Xin H, Takahashi M, Nukiwa T, Hagiwara K. A naturally occurring p73 mutation in a p73-p53 double-mutant lung cancer cell line encodes p73 alpha protein with a dominant-negative function. Cancer Sci. 2003;94(8):718-24.
38. Kaghad M, Bonnet H, Yang A, Creancier L, Biscan JC, Valent A, et al. Monoallelically expressed gene related to p53 at 1p36, a region frequently deleted in neuroblastoma and other human cancers. Cell. 1997;90(4):809-19.
39. Coates PJ. Regulating p73 isoforms in human tumours. J Pathol. 2006;210(4):385-9.
40. Ramadan S, Terrinoni A, Catani MV, Sayan AE, Knight RA, Mueller M, et al. p73 induces apoptosis by different mechanisms. Biochem Biophys Res Commun. 2005;331(3):713-7.
41. John K, Alla V, Meier C, Putzer BM. GRAMD4 mimics p53 and mediates the apoptotic function of p73 at mitochondria. Cell Death Differ. 2011;18(5):874-86.
42. Sayan AE, Sayan BS, Gogvadze V, Dinsdale D, Nyman U, Hansen TM, et al. p73 and caspase-cleaved p73 fragments localize to mitochondria and augment TRAIL-induced

apoptosis. Oncogene. 2008;27(31):4363-72.
43. Kramer S, Ozaki T, Miyazaki K, Kato C, Hanamoto T, Nakagawara A. Protein stability and function of p73 are modulated by a physical interaction with RanBPM in mammalian cultured cells. Oncogene. 2005;24(5):938-44.
44. Nakano H, Shinohara K. Time sequence analysis of caspase-3-independent programmed cell death and apoptosis in X-irradiated human leukemic MOLT-4 cells. Cell and tissue research. 2002;310(3):305-11.
45. Haider N, Narula N, Narula J. Apoptosis in heart failure represents programmed cell survival, not death, of cardiomyocytes and likelihood of reverse remodeling. Journal of cardiac failure. 2002;8(6):S512-S7.
46. Elmore S. Apoptosis: A review of programmed cell death. Toxicol Pathol. 2007;35(4):495-516.
47. Wang XD. The expanding role of mitochondria in apoptosis. Genes Dev. 2001;15(22):2922-33.
48. Wilk S. Teaching resources. Apoptosis. Sci STKE. 2005(285):tr16.
49. Coultas L, Strasser A. The role of the Bcl-2 protein family in cancer. Semin Cancer Biol. 2003;13(2):115-23.
50. Letai A. Pharmacological manipulation of Bcl-2 family members to control cell death. J Clin Invest. 2005;115(10):2648-55.
51. Andreyev AY, Kushnareva YE, Starkov AA. Mitochondrial metabolism of reactive oxygen species. Biochemistry (Mosc). 2005;70(2):200-14.
52. Marchi S, Giorgi C, Suski JM, Agnoletto C, Bononi A, Bonora M, et al. Mitochondria-ros crosstalk in the control of cell death and aging. J Signal Transduct. 2012;2012:329635.
53. Mayer B, Oberbauer R. Mitochondrial regulation of apoptosis. News Physiol Sci. 2003;18:89-94.

54. Szewczyk A, Wojtczak L. Mitochondria as a pharmacological target. Pharmacol Rev. 2002;54(1):101-27.
55. Erro E, Tunon T. [Preliminary results of the study of neuronal death and the expression of bcl-2 protein in Alzheimer's disease]. Rev Med Univ Navarra. 1997;41(1):28-33.
56. Kitamura Y, Shimohama S, Kamoshima W, Ota T, Matsuoka Y, Nomura Y, et al. Alteration of proteins regulating apoptosis, Bcl-2, Bcl-x, Bax, Bak, Bad, ICH-1 and CPP32, in Alzheimer's disease. Brain Res. 1998;780(2):260-9.
57. Paradis E, Douillard H, Koutroumanis M, Goodyer C, LeBlanc A. Amyloid beta peptide of Alzheimer's disease downregulates Bcl-2 and upregulates bax expression in human neurons. J Neurosci. 1996;16(23):7533-9.
58. Lin MT, Beal MF. Mitochondrial dysfunction and oxidative stress in neurodegenerative diseases. Nature. 2006;443(7113):787-95.
59. Seo AY, Joseph AM, Dutta D, Hwang JCY, Aris JP, Leeuwenburgh C. New insights into the role of mitochondria in aging: mitochondrial dynamics and more. J Cell Sci. 2010;123(15):2533-42.
60. Kalous M, Drahota Z. The role of mitochondria in aging. Physiol Res. 1996;45(5):351-9.
61. Papoutsaki M, Lanza M, Marinari B, Nistico S, Moretti F, Levrero M, et al. The p73 gene is an anti-tumoral target of the RAR beta/gamma-selective retinoid tazarotene. J Invest Dermatol. 2004;123(6):1162-8.
62. Lakshmana MK, Chung JY, Wickramarachchi S, Tak E, Bianchi E, Koo EH, et al. A fragment of the scaffolding protein RanBP9 is increased in Alzheimer's disease brains and strongly potentiates amyloid-beta peptide generation. Faseb J. 2010;24(1):119-27.

63. Wan YY, DeGregori J. The survival of antigen-stimulated T cells requires NFkappaB-mediated inhibition of p73 expression. Immunity. 2003;18(3):331-42.
64. Frank S, Gaume B, Bergmann-Leitner ES, Leitner WW, Robert EG, Catez F, et al. The role of dynamin-related protein 1, a mediator of mitochondrial fission, in apoptosis. Dev Cell. 2001;1(4):515-25.
65. Smirnova E, Griparic L, Shurland DL, van der Bliek AM. Dynamin-related protein Drp1 is required for mitochondrial division in mammalian cells. Mol Biol Cell. 2001;12(8):2245-56.
66. Tanaka A, Youle RJ. A chemical inhibitor of DRP1 uncouples mitochondrial fission and apoptosis. Mol Cell. 2008;29(4):409-10.
67. Yu T, Fox RJ, Burwell LS, Yoon Y. Regulation of mitochondrial fission and apoptosis by the mitochondrial outer membrane protein hFis1. J Cell Sci. 2005;118(Pt 18):4141-51.
68. Duckett CS, Li F, Wang Y, Tomaselli KJ, Thompson CB, Armstrong RC. Human IAP-like protein regulates programmed cell death downstream of Bcl-xL and cytochrome c. Mol Cell Biol. 1998;18(1):608-15.
69. Deveraux QL, Reed JC. IAP family proteins--suppressors of apoptosis. Genes Dev. 1999;13(3):239-52.
70. Gogada R, Prabhu V, Amadori M, Scott R, Hashmi S, Chandra D. Resveratrol induces p53-independent, X-linked inhibitor of apoptosis protein (XIAP)-mediated Bax protein oligomerization on mitochondria to initiate cytochrome c release and caspase activation. J Biol Chem. 2011;286(33):28749-60.
71. Findley HW, Gu L, Yeager AM, Zhou M. Expression and regulation of Bcl-2, Bcl-xl, and Bax correlate with p53 status and sensitivity to apoptosis in childhood acute lymphoblastic leukemia. Blood. 1997;89(8):2986-93.

72. Janumyan YM, Sansam CG, Chattopadhyay A, Cheng N, Soucie EL, Penn LZ, et al. Bcl-xL/Bcl-2 coordinately regulates apoptosis, cell cycle arrest and cell cycle entry. Embo J. 2003;22(20):5459-70.
73. Sayan AE, Sayan BS, Gogvadze V, Dinsdale D, Nyman U, Hansen TM, et al. P73 and caspase-cleaved p73 fragments localize to mitochondria and augment TRAIL-induced apoptosis. Oncogene. 2008;27(31):4363-72.
74. Chang LK, Liu ST, Kuo CW, Wang WH, Chuang JY, Bianchi E, et al. Enhancement of transactivation activity of Rta of Epstein-Barr virus by RanBPM. Journal of molecular biology. 2008;379(2):231-42.
75. Poirier MB, Laflamme L, Langlois MF. Identification and characterization of RanBPM, a novel coactivator of thyroid hormone receptors. J Mol Endocrinol. 2006;36(2):313-25.
76. Rao MA, Cheng H, Quayle AN, Nishitani H, Nelson CC, Rennie PS. RanBPM, a nuclear protein that interacts with and regulates transcriptional activity of androgen receptor and glucocorticoid receptor. Journal of Biological Chemistry. 2002;277(50):48020-7.
77. Eckert A, Hauptmann S, Scherping I, Rhein V, Muller-Spahn F, Gotz J, et al. Soluble beta-amyloid leads to mitochondrial defects in amyloid precursor protein and tau transgenic mice. Neurodegener Dis. 2008;5(3-4):157-9.
78. Lakshmana MK, Hayes CD, Bennett SP, Bianchi E, Reddy KM, Koo EH, et al. Role of RanBP9 on amyloidogenic processing of APP and synaptic protein levels in the mouse brain. Faseb Journal. 2012;26(5):2072-83.
79. Dhanasekaran DN, Reddy EP. JNK signaling in apoptosis. Oncogene. 2008;27(48):6245-51.
80. Schuster A, Schilling T, De Laurenzi V, Koch AF, Seitz S, Staib F,

et al. DeltaNp73beta is oncogenic in hepatocellular carcinoma by blocking apoptosis signaling via death receptors and mitochondria. Cell Cycle. 2010;9(13):2629-39.

81. Wetzel MK, Naska S, Laliberte CL, Rymar VV, Fujitani M, Biernaskie JA, et al. p73 regulates neurodegeneration and phospho-tau accumulation during aging and Alzheimer's disease. Neuron. 2008;59(5):708-21.

82. Killick R, Niklison-Chirou M, Tomasini R, Bano D, Rufini A, Grespi F, et al. p73: a multifunctional protein in neurobiology. Mol Neurobiol. 2011;43(2):139-46.

83. Benosman S, Meng X, Von Grabowiecki Y, Palamiuc L, Hritcu L, Gross I, et al. Complex Regulation of p73 Isoforms after Alteration of Amyloid Precursor Polypeptide (APP) Function and DNA Damage in Neurons. J Biol Chem. 2011;286(50):43013-25.

84. Tissir F, Ravni A, Achouri Y, Riethmacher D, Meyer G, Goffinet AM. DeltaNp73 regulates neuronal survival in vivo. Proc Natl Acad Sci U S A. 2009;106(39):16871-6.

85. Talos F, Abraham A, Vaseva AV, Holembowski L, Tsirka SE, Scheel A, et al. p73 is an essential regulator of neural stem cell maintenance in embryonal and adult CNS neurogenesis. Cell Death Differ. 2010;17(12):1816-29.

국문초록

미토콘드리아 매개에 의한 세포자멸사에서 RanBP9 과 P73 의협력적 역할

리우티안

의과학 전공

서울대학교 대학원

지금까지의 많은 연구들은 아밀로이드 전구 단백질(Amyloid Precursor protein, APP)이 효소에 의해 잘려 만들어진 아밀로이드베타(Aβ)의 축적이 알츠하이머병 유발에 필수적인 역할을 한다고 보고하고 있다. 선행연구에서는 버팀목 단백질인 RanBP9은 APP가 BACE1에 의해 잘려 Aβ를 형성하는 현상을 강력하게 증가시킨다고 보고하였다. 또한 RanBP9의 발현은 알츠하이머 환자의 뇌에서 증가되어 있다. 최근 한 연구에 따르면 RanBP9은 DNA 손상에 의한 세포사멸을 증가시키며 RanBP9의 넉다운은 Bax 단백질을 증가시킨다. 그러나 RanPB9이 어떤 기전으로 세포

사멸을 일으키는지에 대해서는 연구가 미흡한 상황이다. 본 연구에서는 RanPB9 과발현이 미토콘드리아 활성산소를 증가시키고 미토콘드리아의 세포막전압을 떨어뜨린다는 사실을 밝혔다. 또한 Annexin V와 LDH분비 실험을 통해 세포사멸이 관찰되지 않는 혈청 회수 상황에서도, RanBP9은 세포사멸을 일으킴을 증명하였다. 이 현상은 Bax가 RNA수준이 아닌 단백질 수준에서 증가한 것과 항 세포사멸 단백질인 Bcl-2 단백질의 감소한 결과에 의해 반증되었다. 면역염색기법을 통해 RanBP9과발현은 미토콘드리아 형태를 망가뜨리며 싸이토크롬 씨의 분비를 일으키는 것을 확인하였다. 흥미롭게도 원래 길이의 RanBP9과 특별히 알츠하이머 환자에서 증가되어 있는 N60 단편이 생화학적으로 분리된 미토콘드리아 부분에서 증가되어 있는데 이것은 RanBP9이 미토콘드리아에서 직접적인 역할을 할 것이라는 것을 시사하였다. 또한 본 연구에서는 RanBP9과 p73α에 의한 세포사멸이 각각 p73 siRNA와 RanBP9 siRNA에 의해 방해됨을 증명하였다. 동시에 p73 siRNA는 RanBP9에 의한 Bax와 Bcl2 단백질의 균형 이상과 비정상적인 미토콘드리아 분열을 회복시켰다. HT22 세포주에서 RanBP9은 p73와 상호작용하였고 미토콘드리아 내의 p73α와 p73

의 양을 증가시켰으며 RanBP9은 p73 단백질의 반감기에 영향을 주었다. 또한 RanBP9 과발현 쥐에서 배양한 해마 신경세포에서는 함께 태어난 야생형의 신경세포에서보다 더 많은 양의 p73이 발현되어 있었다. 이러한 결과는 RanBP9이 Aβ를 증가시키는 역할 이외에도 p73와 함께 미토콘드리아를 통해 세포사멸을 일으켜 알츠하이머 발생에 기여한다는 것을 제시한다.

* 본 내용은Cell Death and Disease 학술지 (Cell Death and Disease (2013) 4, e476; doi:10.1038/cddis.2012.203; published online 24 January 2013)에 출판 완료된 내용임

……

주요어: 아밀로이드; 세포자멸사; RanBP9; p73; 마토콘드리

학번: 2010-31373